Effects of Cell Migration

on Polyethylenimine/pDNA Polyplex

Transfection Efficacy and Mechanism

by

Jacob Dugan Hewes

A thesis submitted to the Faculty of the University of Delaware in partial fulfillment of the requirements for the degree of Honors Bachelor of Chemical Engineering with Distinction

2023

Effects of Cell Migration

on Polyethylenimine/pDNA Polyplex

Transfection Efficacy and Mechanism

by

Jacob Dugan Hewes

Approved: _____
Millicent O. Sullivan, Ph.D.
Professor in charge of thesis on behalf of the Advisory Committee

Approved: _____
Catherine A. Fromen, Ph.D.
Committee member from the Department of Chemical & Biomolecular Engineering

Approved: _____
Chitraleema Chakraborty, Ph.D.
Committee member from the Board of Senior Thesis Readers

Approved: _____
Michael Chajes, Ph.D.
Dean, University Honors Program

ACKNOWLEDGMENTS

I would like to thank my research advisors and mentors, Dr. Millicent Sullivan, and Dr. Norman Wagner. Dr. Wagner provided me with the opportunity to conduct research prior to my senior year of high school through the UD-K12 Engineering Summer Internship Program, and it was under his tutelage that my love for research was born. As a high school student in the Wagner Group, my love for chemical engineering research was born and laid the foundation for me to achieve success in my academic and professional endeavors. Through the three projects I worked on with Dr. Wagner, he instilled in me the skills necessary to conduct my own independent research, and he has continued to serve as an incredible resource and inspiration for my future career. I had always had the goal of developing novel therapeutics to cure disease, so when Dr. Sullivan granted me the opportunity to join her lab focused on biomaterials and drug and gene delivery, I was overjoyed. Through working with Dr. Sullivan, my passion for drug and gene delivery flourished, which will now be the focus of my graduate education. Even when she became chair of the department, she still managed to invest in my growth as a researcher and generally as a student. She consistently challenged me to think critically and has left me with a newfound confidence as I enter the next stage of my life.

I also want to thank the best two graduate students, James Mullin and Jinzhen (Hugo) Hu. Since Dr. Sullivan was the chair of the department, these two quickly became my right-hand men. Having amateur cell culture experience prior to starting my thesis research, there was a learning curve to master the proper techniques needed

to conduct effective research experiments. They were always willing to answer my many, many questions, respond to late night texts, teach me how to perform a certain assay, or give me advice about being a graduate student. I always enjoyed coming in the office and seeing them grinding on their work or yelling over the fume hood to chat with them. These two became not only mentors, but also true friends, and I am grateful for their mentorship during my research journey.

Outside of the Sullivan group, there are so many people at UD that I am grateful for. All the UD Honors College staff have been so supportive in helping me navigate the overwhelming college environment. I especially would like to thank Ann Himelreich for being my "school mom." I will never forget the dozens of hour long chats I had on the couch in her office or simply walking by her door and hearing, "is that Jacob Hewes!" I was sad to see her leave the department, but her affection towards all chemical engineers was not forgotten. Additionally, thanks to everyone in the department that has helped along the way while I have been a Hengineer. My success in the classroom has been the combination of hard work and amazing professors such Dr. Enszer, Dr. Tilton, Dr. Solomon, Dr. Kunjapur, and many, many more! While each of these individuals played an integral part in my undergraduate career, I must express my appreciation for the Little Bob. Despite the fact that it was essentially a concert most days, it gave me a place to temporarily escape from the responsibilities of everyday life while improving my physical health. Following a consistent exercise routine instilled in me discipline that helped me reach my academic and professional goals.

Most importantly, I have to thank my friends and family for always being there for me. I could write a paper the length of this thesis about their impact on my success,

but all I will say is I love them with all my heart. Special thanks to all the YouTube streamers that provided me with a community and a source of entertainment for the late night work sessions. And, most importantly, thank you to my brother, Noah, for being the best big brother, twin, and friend that I could ever ask for.

TABLE OF CONTENTS

LIST OF FIGURES

ABSTRACT

Nonhealing wounds have been the subject of decades of basic and clinical research. Despite new knowledge about the biology of impaired wound healing, little progress has been made in treating chronic wounds, leaving patients with few therapeutic options. The lack of treatments has created a major global burden on the healthcare system and resulted in high health care costs. In the past few decades, the field of nonviral gene delivery has garnered significant interest as one of the most promising strategies for the treatment of chronic wounds. Nonviral vectors have the advantage to deliver genes to target cells without the immunogenic or toxic responses associated with viral vectors, however, limited gene transfer efficacy remains a challenge. This work aims to address these challenge by optimizing the formulation of poly(ethylenimine) (PEI) nanocarriers for effective plasmid DNA (pDNA) delivery. PEI-pDNA polyplexes were synthesized with different N/P ratios to optimize polyplex properties, including size and zeta potential, and used to transfect NIH/3T3 cells *in vitro*. It was found that an N/P ratio of 10 produced the smallest and most positively charged polyplexes, resulting in the highest transgene expression. Furthermore, a simple *in vitro* wound model was developed and employed to study PEI-pDNA polyplex transfection during wound healing. Cells migrating to close the wound were found to be transfected more readily than cells that did not migrate. Additionally, the transfection efficiency in migrating cells was shown to decrease when less growth factors were present in the extracellular environment. Thus, this work demonstrates that PEI can be used to delivery therapeutic DNA and targeted delivery of transgenes to migrating cells during wound healing could serve as a viable strategy to enhance tissue repair and regeneration.

Chapter 1

INTRODUCTION AND MOTIVATION

1.1 Gene therapy

Gene therapy is an intracellular delivery of genomic materials (transgene) into specific cells to generate a therapeutic effect by correcting an existing abnormality or providing the cells with a new function.[1] Different types of gene delivery systems may be applied in gene therapy to restore a specific gene function or turn off a particular gene(s). The ultimate goal of gene therapy is single administration of an appropriate material to replace a defective or missing gene.[2] The first human gene transfer was utilized in 1989 on tumor-infiltrating lymphocytes[3], and the first gene therapy was done on adenosine deaminase (ADA) gene for treatment of patients with severe combined immunodeficiency defect (SCID) in 1990.[4] Although initially the main focus of gene therapy was on inherited genetic disorders, now diverse diseases, including cystic fibrosis, ADA-SCID, emphysema, retinitis pigmentosa, sickle cell anemia, phenylketonuria, hemophilia, Duchenne muscular dystrophy, and some autosomal dominant disorders. Polygenic disorders, different forms of cancers, vascular disease, neurodegenerative disorders, inflammatory conditions, and other acquired diseases are also targets of gene therapy. At present, there are a total of twenty-seven gene therapy products on the U.S. market and hundreds of clinical trials recruiting patients in clinicaltrials.gov. The turbulence of gene therapy in the past three decades has built many lessons-learned opportunities and paved a solid foundation for the recently renewed excitement about the ability of gene delivery systems to tackle some of the most devastating diseases. This rejuvenation has led to a large growth in the gene therapy market, with seventeen of the twenty-seven currently FDA approved products being produced in the past two years. There are different viral and nonviral vectors for gene delivery, but all gene therapy

applications depend on the fact that the genetic material needs to be delivered across the cell membrane and ultimately to the cellular site of action.

1.2 Gene delivery methods

There are numerous challenges to introduce new genetic materials to hosts as a therapeutic for acquired or inherited diseases. Naked DNA molecules do not enter cells efficiently because of their large size and hydrophilic nature due to negatively charged phosphate groups. In addition, they are very susceptible to nuclease-mediated degradation. Therefore, the primary challenge for gene therapy is to develop carriers, commonly referred to as vectors, and physical methods that facilitate gene transfer to targeted cells without degradation of the delivered gene.

1.2.1 Viral-vectors

Viruses have evolved over millions of years to be efficient delivery vehicles for nucleic acids. Viruses mediate efficient gene transfer through their favorable cell uptake and intracellular trafficking machineries. Recombinant viruses such as retrovirus, lentivirus, adenovirus, adeno-associated virus, and herpes simplex virus have been widely utilized as vectors for gene transfer. All viral vector genomes have been modified by deleting some areas of their genomes so that their replication becomes deranged, and it makes them safer. However, viral vectors have several intrinsic drawbacks including difficulty in production, limited transgenic capacity size, limited opportunity for repeated administrations due to acute inflammatory response, and delayed humeral or cellular immune responses.[5] Additionally, other concerns with using viral vectors as gene delivery vehicles are the immunogenicity and oncogenicity. At the University of Pennsylvania, an 18-year-opatient in a viral-vector gene therapy clinical trial for delivering deoxyribonucleic acid (DNA) as a treatment for liver disease died from side effects of the viral vector treatment.[6] The toxicity concerns along with the other disadvantages of viral vectors limits their potential for clinical translation of DNA therapeutics.

1.2.2 Nonviral vectors

Due to the toxicity and manufacturing challenges associated with viral vectors, nonviral vectors have stood as safer alternatives to be applied for gene transfer. For the delivery of pDNA, systems are usually composed of cationic polymers or lipids with the ability to interact with the negatively charged DNA through electrostatic interactions leading to polyplexes and lipoplexes formation.[7] Nonviral vectors have a low immunogenicity, have a low production cost, and can be easily produced on large scale. Another important characteristic of these vectors is the ability to transfer different and large transgenes, being also able to be stored for long periods due to their stability.[8] However, systemic delivery is a real challenge for these nonviral vectors since they need to avoid cellular defense mechanisms that may try to degrade or capture them. Also, when reaching the target tissue, the systems must go cross the tissue and bind specifically to the target cells. After this internalization process, it is further required to surpass intracellular barriers such as the endosomal escape, the cytoplasm traffic, and finally, enter the nucleus.[9] Thus, the ability of nonviral vectors to overcome these barriers will dictate their therapeutic efficiency.

1.3 Cationic polymer nanocarriers for gene delivery

Cationic polymers form condensed complexes with negatively charged DNA through electrostatic interactions that encapsulate DNA and facilitate cell uptake and intracellular delivery. Upon mixing with DNA, these polymers form nanosized complexes, often called polyplexes. Among cationic polymers commonly used for gene transfer, PEI is considered one of the most effective polymer-based transfection agents, which exists in either branched or linear structures. PEI was first used in gene transfer in 1995.[10] PEI has a high density of amine groups of which majority are nonprotonated at physiological pH levels. The nonprotonated amines in the PEI are hypothesized to exert the proton sponge effect, which effectively prevents the acidification of the endosomal pH by taking up and neutralizing the protons that are pumped by ATPase.[11] Ultimately, it leads to an influx of chloride counter ions within the endosome and a

buildup of osmotic pressure that causes the swelling and rupture of the endosomal membrane. The bursting of the endosome releases the nanocarrier into the cytosol.[12]

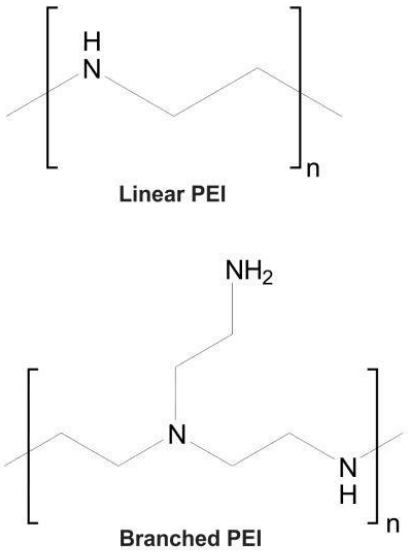

Figure 2-1. Chemical structures of linear and branched polyethylenimine[13]

1.4 Endocytic Uptake.

Endocytosis refers to the energy-dependent cellular uptake of macromolecules and solutes into membrane-bound vesicles derived by invagination and pinching off of the plasma membrane.[14] Engineered nanocarriers can employ similar mechanisms to facilitate entry into the cell through interactions with surface receptors or directly with the plasma membrane. Two main mechanisms for endocytic uptake have been well-characterized: phagocytosis and pinocytosis. In mammalian cells, phagocytosis is conducted primarily by macrophages, monocytes and neutrophiles, to clear large (> 0.5 m) pathogens such as bacteria, yeast, large debris from apoptosis body, dead cells, and arterial fat deposits.[14] In contrast, all cells utilize pinocytosis to regulate uptake of various fluids and solutes via generation of large endocytic vesicles from protrusions in the cellular membrane. Numerous types of pinocytosis have been established, and pinocytic mechanisms often vary depending on cellular origin and function. Pinocytosis contains both non-selective internalization[15] and receptor-mediated mechanisms for cellular uptake. The

two primary classes of receptor-mediated uptake of nanocarriers are clathrin-dependent and caveolae-mediated endocytosis. These processes as well as discussion of how engineering nanocarriers use these mechanisms to facilitate entry into cells are briefly described below.

1.4.1.1 Clathrin-dependent endocytosis

The best characterized route for endocytosis in mammalian cells is that mediated by clathrin, the main protein of specialized membrane structures called clathrin-coated pits (CCPs).[16] Clathrin-dependent endocytosis is an energy-dependent process that begins with binding of ligands to cell surface receptors, leading to localization of these receptors in CCPs on the plasma membrane. The CCPs are constitutively composed by the assembly of clathrin as a polygonal lattice underlying to the membrane, and adaptor protein complexes which mediate the assembly of the clathrin-lattice on the cytosolic face of the plasma membrane.[17] The CCPs containing the ligand-receptor clusters then invaginate and are pinched off from the plasma membrane by dynamin, creating intracellular clathrin-coated vesicles (CCVs) ranging in size from 10 to 200 nm depending on the cell type and payload.[18] Once internalized, the clathrin coat is rapidly depolymerized and recycled back to the plasma membrane. The resulting vesicles fuse with each other to form early endosomes and the endosome lumens become slightly acidic (pH 6.0). Carrier vesicles are formed from early endosomes and are transported along the actin and tubulin cytoskeletal networks to the appropriate cellular location. During transport, proteins, lipids, and other ligands are returned to the plasma membrane and exported out of the cell through exocytosis to maintain membrane integrity. Early endosomes then fuse with late endosomes, which transport encapsulated cargoes to lysosomes with a further reduction to pH 5 during progression from late endosomes to lysosomes.[19] Any remaining endocytosed material is degraded by the acidic environment and digestive enzymes. Engineering nanocarriers that utilize this pathway encounter two critical barriers that impede their therapeutic efficacy: lysosomal degradation and/or entrapment in endosomal vesicles.

1.4.1.2 Caveolae-mediated endocytosis

Caveolae were classically described as flask-or omega-shaped plasma membrane invaginations, with a diameter of 50-60 nm. Biochemical studies discovered that caveolae, currently referred to as lipid rafts, are hydrophobic, detergent-resistant membrane domains rich in cholesterol and sphingolipids that are present in many eukaryotic membrane, particularly in muscle, endothelial, and fibroblast cells. Mechanisms of caveolar uptake were initially discovered by following the trafficking patterns of the SV40, Ebola Zaire, and Marburg viruses[20,21], but other pathogens have also been shown to enter cells using this pathway.[15] Activation of this pathway is both dynamin and actin dependent.[22] Ingestion occurs through vesicular budding of caveolar from the plasma membrane into vesicles about 50 nm in diameter containing caveolin-1. Caveolar vesicles can fuse with early endosomes and traffic through acidifying pathways leading to lysosomes. Alternatively, uptake via caveolae can be done using a non-acidic, non-digestive process, unlike clathrin-medicated endocytosis. In this pathway, caveolae can fuse with neutral vesicular structures known as caveosomes.[23] Caveosomes do not undergo acidification and can avoid fusion with lysosomes.[24] Transport through caveosomes allows nanocarriers to traffic through the Golgi and/or endoplasmic reticulum, avoiding digestive degradation.[25] The inherent innate ability to avoid lysosomes makes the caveolar uptake pathway an appealing target when delivering biologics. Different classes of nanocarriers have been shown to use caveolae-medicated uptake as their primary endocytic mechanism.[26,27] Despite this benefit, engineering nanocarriers and their packaged cargoes must still escape these endocytic vesicles in order to effectively reach their therapeutic intracellular target.

1.5 Intracellular barriers for nonviral gene delivery

During delivery to target sites within the cell, engineered nanocarriers face a multitude of intracellular barriers that limit their ability to fully realize their therapeutic potential. Nanocarriers must first gain access to the interior of target cells through nonspecific methods, such as adsorptive endocytosis, or specific methods such as receptor-mediated endocytosis.[28]

They then must subsequently break free of endosomal compartments by physically destroying the lipid bilayer that sequesters the DNA vectors from the cytoplasm. Alternatively, vectors can include a phenomenon known as the "proton-sponge effect," which disrupts endosomes using osmotic forces indirectly.[11] Endosomes transport cargoes to many destinations within the cell, and as part of this process, ultimately fuse with other compartments such as lysosomes, where their contents are subsequently degraded by digestive enzymes. Prior studies have found that most endocytosed vectors fail to escape endocytic vesicles[29] and many are observed to eventually traffic to lysosomes. This results in degradation, disassembly, or recycling of vectors prior to reaching their desired intracellular target, lowering their therapeutic efficacy.[14] Upon release from endocytic vesicles, the next step for unpackaged DNA molecules or engineered nanocarriers may be to travel through the cytoplasmic space filled with viscous protein solution and a network of cytoskeleton matrix toward the perinuclear region. Nonviral vectors may physically transport the DNA through the nuclear pore complex (NPC) using nuclear location sequences (NLS) that are associated with the transgene DNA or by unpackaging the DNA at the start of the nuclear pore complex so that the free DNA can gain access. For replicating cells, most DNA molecules enter the nucleus through the process of dissolution and reorganization of the nucellar envelope during mitosis.[30] Finally, nanocarriers needed to unpackage the DNA to allow for the transcription machinery to access the DNA and synthesize the therapeutic protein. Cationic lipids dissociate from DNA through lipid mixing and exchange with host cell lipids at the cytoplasm entry step, while DNA complexes formed with cationic polymers, such as PEI, remain stable after endosome escape. The need to overcome these intracellular challenges may require further research to determine rate-limiting steps for particular gene carriers, which will lead to rational design of novel vectors.

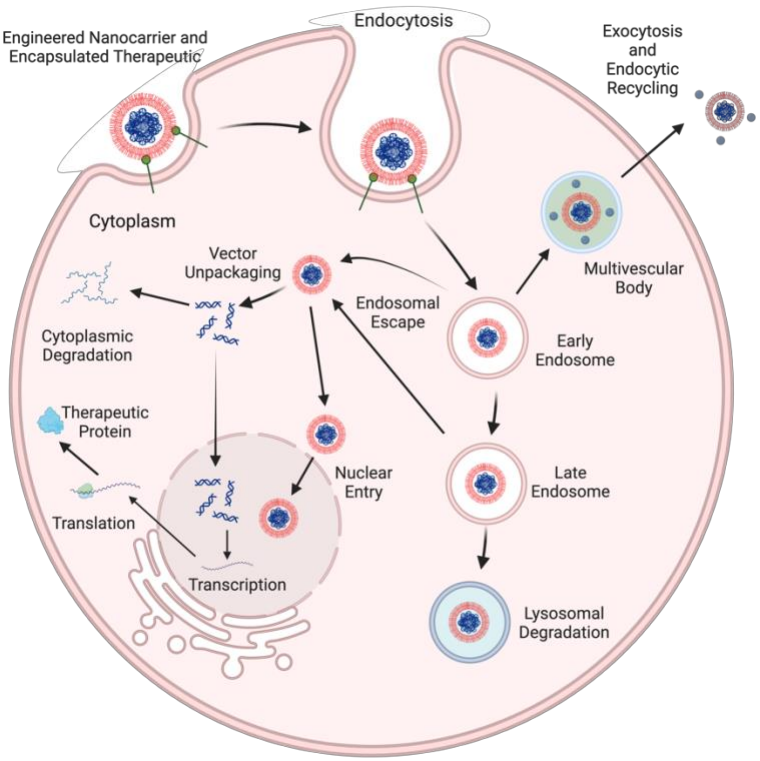

Figure 1-2. Intracellular trafficking of engineered nanocarriers and their therapeutic cargos following endocytosis.

1.6 Thesis Summary

The work herein uses a polyethylenimine polyplex system to explore efficient and controlled methods of gene delivery for wound healing applications by pursuing three specific research aims:

1) Optimize the formulation of polyethylenimine/pDNA polyplex systems for efficient gene delivery
2) Develop a simple *in vitro* wound model for studying cell migration during gene delivery
3) Characterize the effect of cell migration and expression of migratory signals on polyethylenimine/pDNA polyplex transfection

The materials and methods used in this research are outlined in Chapter 2. Advances made towards Research Aim 1 are discussed in Chapter 3. Therein, the process of mixing 25 kDa branched polyethylenimine with plasmid DNA is optimized to achieve polyplex sizes and

surface charges suitable for endocytic uptake and high transfection efficiency of packaged DNA. Furthermore, the properties Chapter 4 discusses approaches towards Research Aims 2 and 3. A convenient and inexpensive *in vitro* model for a healing wound is developed and utilized to study polyethylenimine-based polyplex transfection during the wound healing process. Suggestions for future directions to characterize the endocytic trafficking and reduce the cytotoxicity of PEI/pDNA polyplexes, improve the simplistic wound model, and determine the influence of endolysosomal internalization and trafficking during cell migration on polyplex transfection are suggested. The work herein makes several advances towards improved understanding of DNA delivery during the wound healing process with polyplex gene delivery systems.

Chapter 2

MATERIALS AND METHODS

2.1 Materials

25 kDa branched Polyethylenimine (PEI) (M_n = 10,000 g mol-1, n = 7.9) was obtained from Sigma-Aldrich (St. Louis, MO). The gWIZ plasmid, which encodes for green fluorescent protein (GFP), was purchased from Genlantis (San Diego, CA), amplified in DH5α Escherichia coli, and purified with a ZymoPURE™ II Plasmid Maxiprep Kit (Zymo Research Corp., Irvine, CA) in accordance with the manufacturer's protocols. Dulbecco's modification of Eagle's medium (DMEM) and PBS (150 mM NaCl) were obtained from Corning Life Sciences – Mediatech Inc. (Manassas, VA). Opti-MEM® media was purchased from Thermo Fisher Scientific (Waltham, MA).

2.2 Methods

2.2.1 Polyplex preparation

Polyplexes were formulated via self-assembly method by using solution mixing followed by gentle vortexing. Solutions of pDNA were prepared at 20 μg mL^{-1} in 20 nM 4-(2-hydroxyethyl)piperazine-1-ethanesulfonic acid (HEPES) buffer at pH 6.0. Polymer solutions were prepared in HEPES buffer by adding appropriate amounts of PEI to vary the molar charge composition of the polymer as desired. The polymer solution was added to equal volumes of pDNA solutions to achieve the desired total N/P ratios (N: amine groups on polymer, P: phosphate groups on pDNA). The polymer solution was slowly added while gently vortexing over a period of 10 s. Polyplexes were incubated for 15 min at room temperature before performing additional experiments.

2.2.2 Polyplex Characterization

2.2.2.1 Ethidium bromide gel electrophoresis

Polyplexes were formulated as described and subjected to gel electrophoresis. 1 wt.% agarose gels containing 0.5 μg ethidium bromide mL^{-1} were formed in formed in 1× tris/borate/ethylenediaminetetraacetic acid (EDTA) (TBE) buffer. To analyze polyplexes, 20 μL of polyplex solution was added to 5 μL of gel loading solution (3:7 (v/v) glycerol/water) before being added to the wells. Gels were run at 100 V for 1 hour and imaged using a Bio-Rad Gel Doc XR (Hercules, CA). ImageJ software was used to analyze the amounts of free pDNA by analyzing the intensities of the fluorescent pDNA bands in the gel.

2.2.2.2 Dynamic light scattering

Polyplex solutions were prepared as described and diluted with HEPES buffer to a volume of 1 mL. The solutions were then transferred to a cuvette and analyzed using a Brookhaven Instruments (Brookhaven, CT) ZETAPals with the 90Plus addition. Experiments were performed with a 658 nm wavelength solid-state laser at an angle of 90° and a temperature of 25 °C. For each sample measurement, the hydrodynamic diameter was determined by an intensity-weighted analysis on the data from 3 runs of 2 minutes each.

2.2.2.3 Determining charge with zeta potential

Polyplex solutions were prepared as described and diluted with HEPES buffer to a volume of 1 mL. The solutions were then transferred to a cuvette and analyzed using a ZetaPALS zeta potential analyzer from Brookhaven Instruments (Brookhaven, CT). The samples were measured at 25 °C, and the Smoluchowski model was used to analyze the data. Reported values were computed as the average of three independent experiments comprising 10 measurements each.

2.2.3 Cell culture and transfection

NIH/3T3 cells were purchased from the American Type Culture Collection (ATCC, Manassas, VA). The cells were cultured in DMEM supplemented with 10 vol% fetal bovine serum and 1 vol% penicillin-streptomycin. The cells were maintained at 37 °C in a humidified environment with 5 vol% CO2. For transfections, cells were plated in 12 well plates at a density of 75,000 cells per well. The cells could adhere and recover for 24 h. In preparation for transfection, DMEM was removed, PBS was added in a wash step, and Opti-MEM® reduced serum media was added. Polyplex solutions at a given N:P ratio were added to a final pDNA concentration of 20 nM, and the cells were incubated for 2 h. After the incubation period, the transfection media was removed and replaced with fully supplemented DMEM for the remainder of the culture duration. Transfection efficiencies were measured using fluorescence microscopy and ImageJ.

2.2.4 Wound Healing Scratch Assay

2.2.4.1 Without Transfection

Cells were seeded in a 12-well plate at a density of 75,000 cells per well and grown until confluence at 37°C in complete DMEM containing 10 vol% fetal bovine serum (FBS) and 1 vol% penicillin-streptomycin. Prior to seeding, to obtain the same field during image acquisition, a horizontal line was drawn on the bottom of each well with an ultrafine tip marker. After incubation, a linear scratch was made in the cell monolayer with a 200 μL sterile pipette tip (Thermo Fisher Scientific, Waltham, MA). The cell debris was removed by washing with PBS, and the medium was replaced with 1 mL of fresh medium. Initial images of each scratch were captured using a LSM 780 confocal microscope (Carl Zeiss, Oberkochen, Germany) using a 488 nm laser and a 5x objective. After 24 and 48 hours, images were photographed of each well. To quantify the proliferation and/or migration of cells, the difference between wound width at time 0 and each time period was determined. Scratch width was measured using ImageJ

software. Cell proliferation/migration rate was calculated as percent closure of the scratch a given amount of time:

$$Migration\ Rate = \frac{\left(gap\ distance_{t_0} - gap\ distance_t\right)}{gap\ distance_{t_0}}$$

2.2.4.2 With Transfection

Cells were grown to create a uniform monolayer in a marked dish as previously described. Following wounding and washing with PBS, 0.8 mL of Opti-MEM® and 0.2 mL of polyplex solution were added dropwise throughout each well. Time 0 images were captured, and the dish was then allowed to incubate at 37°C for 2 hours. After the incubation period, the transfection medium was removed and 1 mL of fully supplemented DMEM was added to the cells. The dish was then incubated for 48 hours, and phase-contrast and fluorescence images of each scratch were acquired after 24 and 48 hours. Transfection efficiencies were measured using fluorescence microscopy and ImageJ.

2.2.5 Migratory Transfection Analysis

To quantify transfection efficacy of PEI polyplexes in migratory cells vs. non-migratory cells, the scratch widths between phase-contrast images taken at 0 and 24 hours following transfection were measured using ImageJ. Using the difference in scratch width, the area of each well containing cells that migrated to close the wound was determined and the area containing cells that did not participate in wound closure was found. ImageJ software was used to quantify the integrated fluorescence intensity for each area. The data was then normalized to the non-migratory integrated florescence intensity to enable easy comparison. Integrated fluorescence intensity is computed by ImageJ using the equation shown below. Data for six independent samples was used for each analysis.

$$Integrated\ Density = (Area) * (Mean\ Fluorescence\ Intensity)$$

2.2.6 Wound Scratch Assay with Transfection Using Reduced Growth Factors

DMEM with no supplements was aliquoted into a 50 mL conical tube. 100 µL of fetal bovine serum (FBS), or 0.2 vol%, and 1 vol% penicillin-streptomycin was then added to the media. The procedure for performing a wound scratch assay with transfection was followed as described above, but following the polyplex incubation period, the transfection medium was replaced with DMEM supplemented with 0.2 vol% FBS rather than 10 vol%. The dish was then incubated for 24 hours, and phase-contrast and fluorescence images of each scratch were acquired. Transfection efficiencies were measured using fluorescence microscopy and ImageJ.

2.2.7 Statistical Analysis

A Student's t test was utilized to determine significant differences in sample populations.

Chapter 3

FORMULATION DESIGN OF POLYETHYLENIMINE-BASED NANOCARRIERS

3.1 Background and motivation

3.1.1 Polyethyleneimine-based Polyplex Nanoparticles

Polyethylenimine (PEI) is the organic macromolecule with the highest cationic-charge-density potential. Every third atom is an amino nitrogen that can be protonated. Acid-catalyzed polymerization of aziridine produces a highly branched network that can capture DNA, and, owing to the close neighborhood of the many linker amino groups, PEI retains a substantial buffering capacity at virtually any pH. This simple molecular property is related to the efficiency of the complex multistage process of transfection. Due to the efficiency of PEI as a vector for delivery of oligonucleotides and plasmids both *in vitro* and *in vivo*, PEIs and their derivatives have already been used for the delivery of genetic material into cells in culture and for the development of methods for the treatment of genetic and cancer diseases.[31] The properties of these vehicles depend on the size, dispersity, and hydrophilicity of the used polymer and ratio of polymers in the complex, which are responsible for the size, surface charge, and hydrophilicity of the resulting nanoparticles.

3.1.2 Formulation of Polyplex Nanoparticles

DNA undergoes a large volume transition, known as condensation, when complexed with polycations to form polyplexes, which give rise to decreasing its volume by about 1000 fold. This reduction in volume is essential for genomic DNA packaging. The mechanism of DNA condensation can be described as follows.[32] DNA in water assumes an expanded coil conformation due to the charge repulsion between phosphate groups residing along the chain. When polycations are added, DNA and the polycations form an ionic pair for charge neutralization. This is driven by the entropy gained from the release of counterions bound to both polyelectrolytes into the bulk solution.[33] The charge-neutralized polyion pair undergoes chain

rearrangement to reduce the unfavorable surface area in contact with water molecules, resulting in a volume transition into a compact form. Subsequently, the polyplexes undergo secondary association to further reduce their surface area, grow into multimolecular aggregates, and ultimately precipitate. The amount of polycations required to induce the volume transition largely depends on the number of their charges.

The mixing of polycations with DNA in different ratios, which are most often expressed as the ratio of the number of polycation amino groups (N) to the number of phosphate groups of DNA (P), can afford complexes with different charges and sizes. At low N/P ratios, complexes between transgene DNA and polycations such as PEI have been shown to cause an insignificant decrease in the hydrodynamic size of DNA and poorly protect DNA from enzymatic degradation in biological fluids, resulting in low efficiency of transfection with such complexes. At an N/P ratio close to unity, neutral complexes prone to aggregation are formed. Stable complexes are produced at N/P ratios not lower than 2-3.[34] However, even at such ratios, these complexes are prone to aggregation in due course via hydrophobic interactions and van der Waals forces.[35] The stability of polyplexes increases with increasing N/P ratio due to an increase in the electrostatic repulsion of the complexes, the surface potential of which takes rather high values in complexes of DNA with PEI.[36] Increasing the N/P ratio leads to a decrease in the size of the complexes,[37] however, the fraction of PEI in the free form also increases, leading to an increase in cytotoxicity. An excess of free PEI is necessary for more efficient transfection of cells as the additional PEI prevents undesirable interactions of the polyplexes with glycosaminoglycans on the surface of transfected cells and hinders the premature unpacking of DNA.[38] The purification of suspensions of polyplex nanoparticles from an excess of PEI using different methods led to the reduction of the cytotoxicity but also decreased the efficiency of transfection of cells in culture.[39]

3.2 Research Aim 1 - Optimize the formulation of polyethylenimine/pDNA polyplex systems efficient for gene delivery

This chapter discusses efforts to formulate PEI-based polyplexes with conventional vortex mixing to optimize PEI-pDNA complex properties such as size, zeta potential, and polydispersity that enable efficient pDNA delivery efficiency *in vitro*. Figure 3-1 depicts a schematic representation of the formation of PEI-pDNA polyplexes. Polyplexes were characterized by their N/P ratio. It was found the higher N/P ratio polyplexes, or those with a higher ratio of PEI to pDNA, were smaller in size and more positively charged than complexes of lower N/P ratios. Additionally, polydispersity of the PEI-pDNA nanocarriers was found to be largest at low and high N/P ratios, exhibiting a nonlinear relationship with the N/P ratio. Furthermore, N/P 10 polyplexes were shown to have the highest transfection, but also shown to exhibit more toxic effects than the larger, less positively charged nanocarriers. The work in this chapter demonstrates promising efforts towards Research Aim 1 for this project.

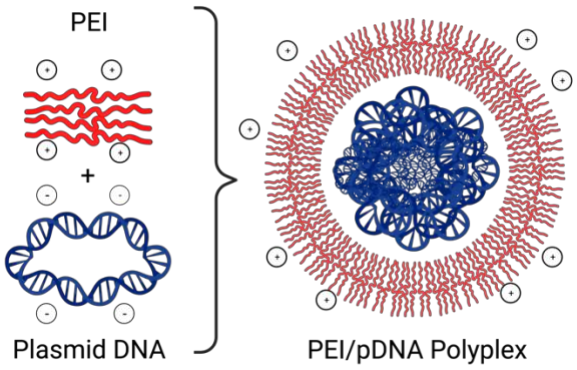

Figure 3-1. Schematic representation of the PEI-pDNA polyplex formulation utilized in this work. Blue indicates pDNA and red indicates 25 kDa branched polyethylenimine.

3.3 Results and Discussion

3.3.1 PEI polyplex pDNA encapsulation

Efficient binding and encapsulation of pDNA is required for a polymer delivery vehicle to protect pDNA from being damaged or degraded before cellular uptake.[40] To analyze the encapsulation abilities of the PEI-pDNA polyplexes, ethidium bromide gel electrophoresis

assays were conducted. As shown in Figure 3-2, polyplexes with a larger N/P ratio were more effectively encapsulated pDNA. The free plasmid DNA that served as a control had fluorescent bands corresponding to nicked (circular), linear, and supercoiled DNA. At an N/P ratio of 4 and 6, there is the presence of free pDNA while the N/P 10 polyplexes were fully able to encapsulate all the pDNA. This aligns with previously observed trend of enhanced encapsulation ability for polyplexes with larger N/P ratios, or more PEI.[40] For future transfections, all polyplexes were made with an N/P greater than 6 to ensure encapsulation of the pDNA.

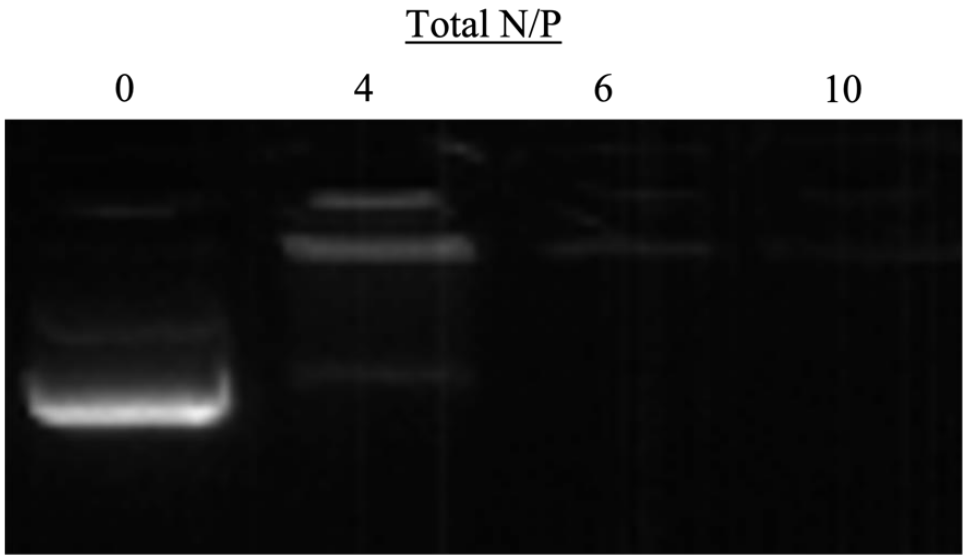

Figure 3-2. Gel electrophoresis assay of PEI-pDNA polyplexes formed at varying N/P ratios. An N/P ratio of 0 represents free plasmid DNA that served as a control.

3.3.2 Polyplex Size and Charge

The extent of cellular uptake and transgene expression has been reported to be dependent on the size and zeta potential of the nanocarrier, which are both influenced by the N/P ratio.[41] The hydrodynamic diameter of PEI polyplexes has been shown to decrease as the N/P ratio increase, but levels off after about a N/P ratio of 5. Additionally, the zeta potential of the nanocarrier was also reported to increase with N/P ratio, but only increases minutely after an N/P of 5.[42] Improvements in transfection efficiency of PEI polyplexes has been demonstrated for

smaller complexes with larger surface charges. Thus, it was hypothesized that polyplexes with a larger N/P ratio would yield smaller particles with more positive surface charges. Using dynamic light scattering, the average diameter of PEI polyplexes with N/P ratios of 4, 6, and 10 was measured. As shown in Figure 3-3, an N/P ratio of 4 produced the largest average polyplex diameter while an N/P ratio of 10 yielded the smallest polyplexes with an average diameter of 98.4 nm. This was consistent with DLS measurements reported previously.[43] Entry in the intracellular compartment will be simplified if the delivery system has a diameter less than 200 nm since these nanocarriers will be mostly internalized via clathrin-mediated and caveolae-mediated endocytosis.[44] Complexes between 250 nm and 3 µm have been shown to have an optimal *in vitro* uptake by micropinocytosis and phagocytosis, producing lower transgene expression than receptor-mediated uptake.[45] Therefore, polyplexes with a higher N/P ratio, corresponding to a greater amount of PEI, would be expected to be internalized more efficiently, primarily utilizing receptor-mediated uptake pathways. On the other hand, polyplexes at lower N/P ratios would likely be endocytosed through micropinocytosis and phagocytosis.

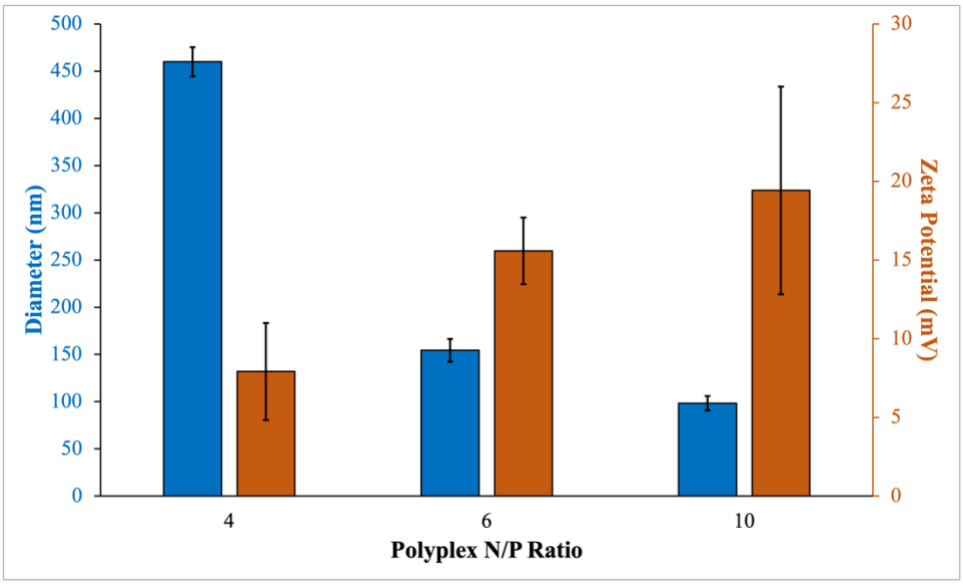

Figure 3-3. Average hydrodynamic diameters (blue, associated with the primary y-axis) and zeta potentials (orange, associated with secondary y-axis) of polyplexes with varying N/P ratios. Results are shown as the mean ± standard deviation of data obtained from three independent measurements.

A positive surface charge is a critical requirement to be considered for any carrier to be used as an efficient gene delivery system. The positive charge promotes nanoparticle interaction with anionic glycosaminoglycans on the cell surface and enhances their uptake.[46] The zeta potential can be used to determine whether a charged active material is encapsulated within the center of the polyplex or on the surface. Thus, the zeta of the various pDNA-loaded polyplexes was evaluated. The zeta potential was measured for each formulation and is plotted in Figure 3-3. The positive zeta potential values indicate that all the polyplexes had an overall positive net charge. The linear relationship between zeta potential and N/P ratio was expected since larger amounts of PEI, which contains a high positive-charge density, are used in higher N/P polyplex compositions. Considering the results obtained, it can be suggested that these polyplexes essentially created a "shell" made essentially of polymer being the genetic information fully protected inside the carriers.

Successful formulation of safe, stable, and efficient nanocarriers for *in vitro* and *in vivo* applications requires the preparation of homogenous populations of nanocarriers with defined and predictable characteristics. Thus, the polydispersity of the formulated polyplexes was measured. The polydispersity index (PDI) is essentially a representation of the distribution of size populations within a given dispersion. It typically ranges from values of 0.0 to 1.0, the latter suggesting a highly polydisperse dispersion with multiple particle sizes present. PDI values <0.2 indicate that most complexes formed are narrowly dispersed without significant aggregation and are most commonly deemed acceptable in practice.[47] As shown in Figure 3-4, the PDI of N/P = 4 polyplexes was the largest, followed by N/P = 10 and N/P = 6, respectively. The large PDI at lower N/P ratios could be related to the initially formed polyplexes since these complexes tend to agglomerate due to the lower surface charge of the polyplexes. On the other hand, a large PDI at higher N/P ratios could be produced by interactions through the accessible unbound DNA chains in one polyplex with the unbound PEI of another polyplex, resulting in some aggregation.[45] All of the polyplexes had PDIs larger than 0.2, indicating that these preparations would be to polydisperse to be used for *in vivo* applications.

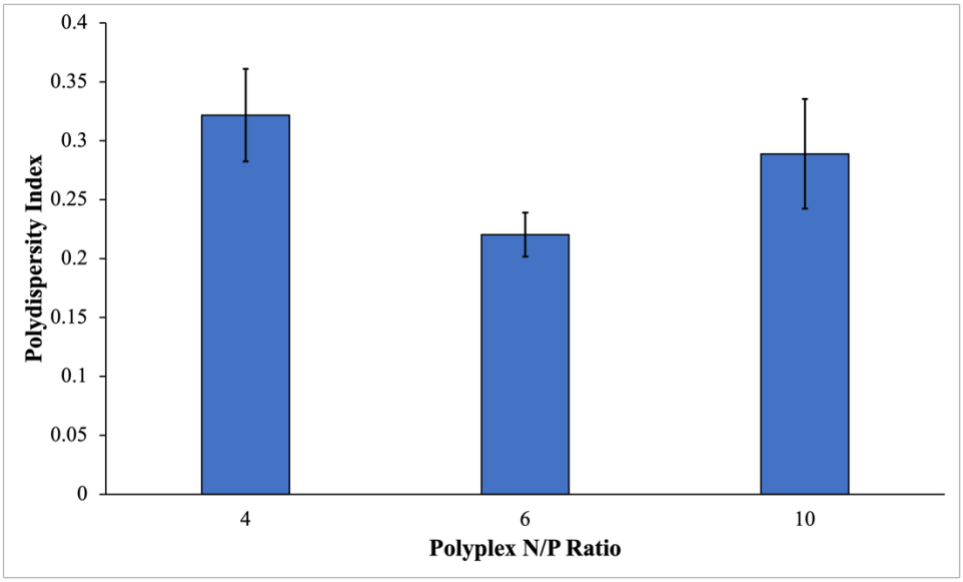

Figure 3-4. Average polydispersity indexes of polyplexes with varying N/P ratios. Results are shown as the mean ± standard deviation of data obtained from three independent measurements.

As mentioned above, the entry of large particles into the cell it is not easy, and their structure is not stable enough to resist the low pH environment and lysosomal enzymes.[48] Thus, the complete characterization and selection of suitable nanocarriers must include the evaluation of the biological response of the cells transfected with the polyplexes produced. In this case, the biological effect was assessed for the PEI-based polyplexes that presented the best values in terms of zeta potential and hydrodynamic size. These conditions led to the selection of the N/P ratio of 10 for PEI-based polyplexes. Additionally, the transfection efficiency of N/P 10 polyplexes was compared to polyplexes with lower N/P ratios to determine whether the smaller particles with more surface charge correspond to better therapeutic efficacy.

3.3.3 Cell Transfection

48 hours following transfection, the transfection efficiencies of PEI−pDNA polyplexes with an N/P ratio of 10 were analyzed by fluorescence microscopy. As seen in Figure 3-5, polyplexes formed at an N/P ratio of 10 produced a significant number of GFP-expressing cells. Thus, these complexes produced from pDNA and a cationic polymer were readily taken up by

cells via endocytosis. Although endocytosis is a barrier to achieving gene delivery, intracellular trafficking has been suggested to be the main challenge that affects transfection efficiency.[49] The notable GFP expression seen for the N/P 10 polyplexes also demonstrates that these vectors induced endosomal release, transported through the cytoplasm, were transferred into the nucleus, and unpackaged their genetic cargo. Previous studies regarding the uptake mechanisms for PEI nanoparticles indicate that PEI polyplexes significantly utilize both clathrin- and caveolae-mediated endocytosis for cellular uptake in NIH/3T3 cells.[14] PEI is best known for its capacity to initiate gene transfer following endolysosomal trafficking, which can be attributed to use the proton sponge effect. The endolysosomolytic activity of PEI is attributed to its buffering capacity and to use the proton sponge effect to rupture the endosome. Further studies are needed to unveil the influence of clathrin- and caveolae-mediated pathways for pDNA delivery to NIH/3T3 cells.

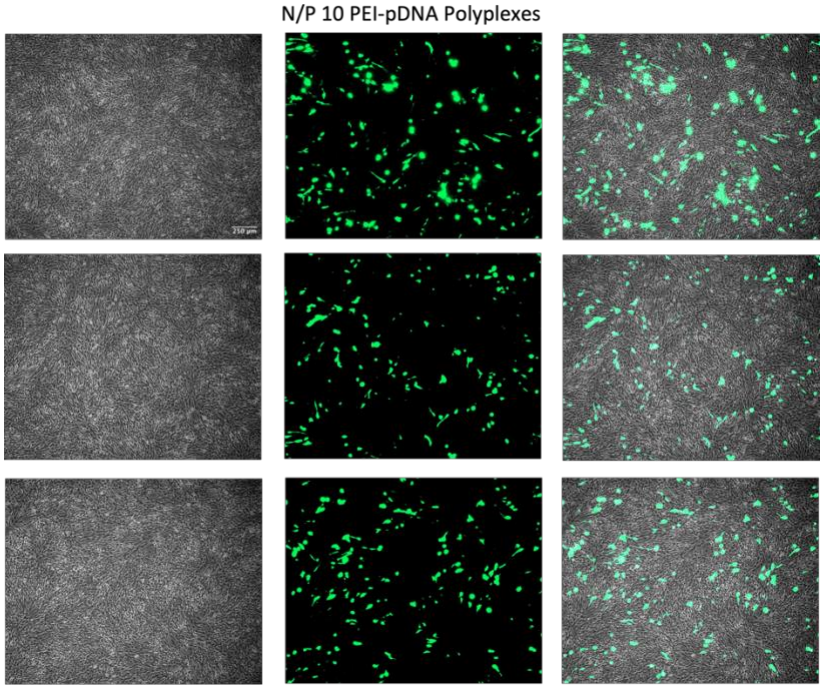

Figure 3-5. Transfection efficiencies of PEI-pDNA polyplexes 48 hours post-transfection. Representative phase contrast microscopy (left), fluorescence microscopy (middle), and overlay (right) images of cells following transfection with N/P 10 polyplexes. The scale bar (shown in top left image) = 250 μm.

After observing significant transfection using N/P 10 polyplexes, the transfection efficiencies of polyplexes formed at lower N/P ratios were also analyzed and compared to the N/P 10 complexes to observe the effect of N/P ratio on gene expression. PEI-pDNA polyplexes were formed at N/P ratios of 6, 8, and 10 following the protocol described in chapter 2. NIH/3T3 cells were transfected and 24 hours following transfection, phase contrast images were captured to analyzed transfection efficiency. As seen in Figure 3-6, polyplexes with higher N/P ratios transfected a larger number of cells compared to those at lower N/P ratios. This can be explained by the fact that polyplexes with lower N/P ratios are larger, making endocytosis by clathrin- or caveolae-mediated uptake less likely to occur. Furthermore, lower zeta potentials and polymer composition makes endolysosomal escape for internalized complexes more challenging, resulting in lower rates of gene transfer. Thus, for all future studies, polyplexes were formulated at an N/P ratio of 10 to promote efficient gene transfer.

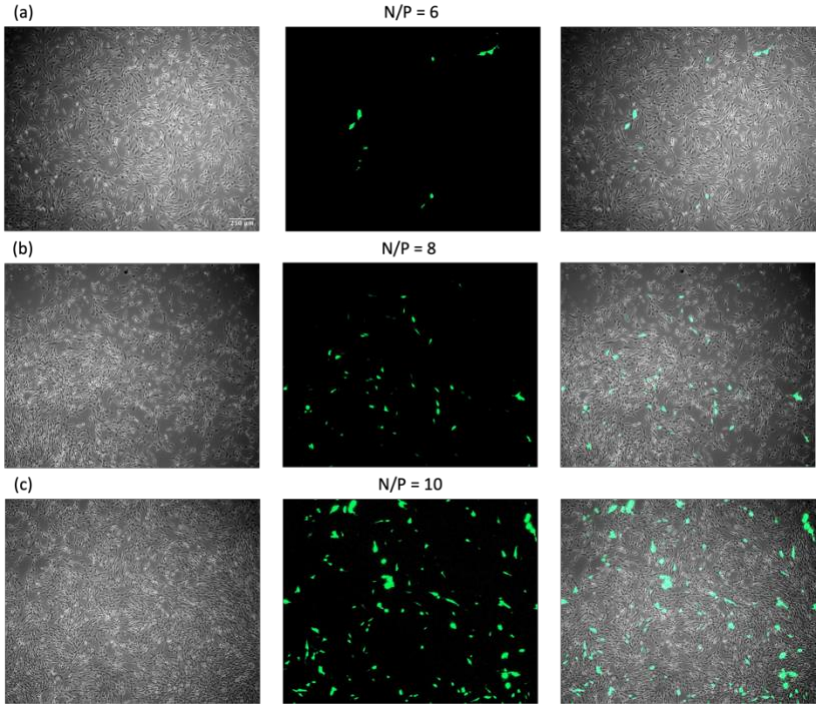

Figure 3-6. Transfection efficiencies of PEI-pDNA polyplexes 24 hours post-transfection. Phase contrast microscopy (left), fluorescence microscopy (middle), and overlay (right) images of cells following transfection with the indicated polyplexes. The scale bar (shown in top left image) = 250 μm.

3.3.4 Cell Viability

While PEI is one of the most efficient nonviral gene delivery vectors due to its high DNA-condensing ability, application of PEI for gene delivery into target cells can be restricted by drawbacks such as high cytotoxicity and unspecific interactions with normal cells or blood components *in vivo*. Charged polycations such as PEI can nonspecifically interact with the negatively charged cell surface in culture or with the vessel walls in the body. This can cause toxicity concerns at high concentrations, which are more pronounced as polymer molecular weight increases due to cell necrosis resulting from disruption of the cell membrane.[50] The toxicity of PEI at high concentrations is primarily due to its interaction with syndecans on the cell surface.[51] At lower concentrations, PEI can activate the apoptosis pathway by damaging mitochondrial membranes, releasing the electron transport chain and cytochrome C.[50] In systemic administration of PEI-pDNA complexes, PEI is rapidly released from the bloodstream and is accumulated in the liver and spleen,[51] where necrotic foci are observed at high PEI concentrations.[52] Additionally, aggregation of large doses of polyplexes resulting from interaction with protein and blood cells leads to obstruction of pulmonary capillaries along with toxic effects.[53]

Figures 3-5 and 3-6 shows that 25 kDa branched PEI exhibits high transfection efficiency, but higher levels of PEI in higher N/P ratio complexes can result in lower cell viabilities. Thus, a tradeoff exists between toxic effects and therapeutic efficacy. Prior work by the group exploring polyplexes synthesized with histone H3 tail peptides containing transcriptionally activating modifications and PEI evaluated the cytotoxicity of PEI-pDNA complexes in Chinese hamster ovary (CHO) cells.[43] 24 hours following transfection, cells were stained with ethidium homodimer-1 (EthD-1) and imaged with fluorescence microscopy.

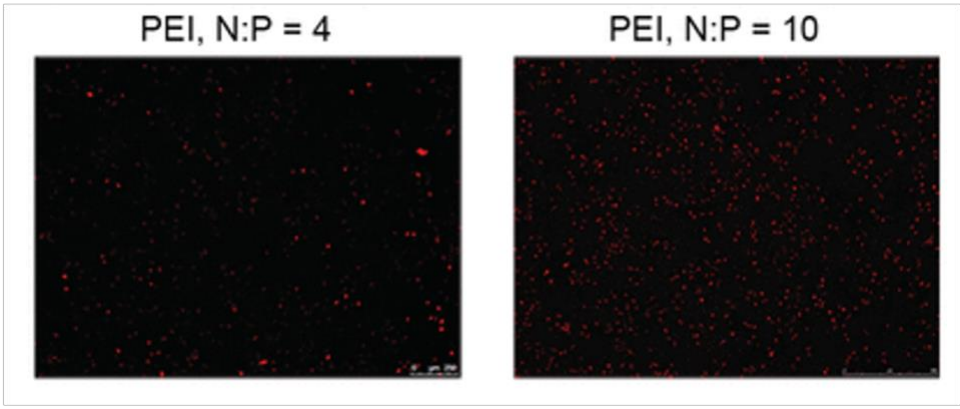

Figure 3-7. CHO cell viabilities 24 hours after polyplex-mediated transfection. Representative fluorescence microscopy images of EthD-1-stained cells. Figured reprinted and adapted from Reilly et. al.[43] The scale bar (shown in the left image) = 250 μm.

As seen in Figure 3-7, the amount of red increased proportionately in the presence of more PEI, i.e., at higher N/P ratios. Cell viability at a higher N/P ratio (N/P = 10) was significantly compromised, which is consistent with previous studies using PEI as the polymer delivery vehicle.[54] At lower charge ratios (N/P = 4), transfection with PEI maintained reasonably high cell viability. However, these polyplexes produced very low transfection efficiency. Thus, to utilize PEI-based polyplexes for therapeutic applications *in vivo*, methods are needed to reduce the toxicity, aggregation, and non-specific interactions while harnessing the transfection ability of PEI. Many strategies, such as PEGylation, bonding PEI with functional groups and synthesis of biodegradable PEIs through crosslinking or grafting, have been successfully used to reduce cytotoxicity and promote the transfection efficiency of PEI.[55] Previous work by the group showed that incorporation of histone H3 tail peptides, in combination with PEI, produced efficient *in vitro* cell transfection without compromising cell viability. The PEI promoted efficient cellular uptake while the H3 peptide enhanced transfection. Future research will explore modifications of the PEI-pDNA polyplexes to reduce cytotoxicity while maintaining high levels of transfection.

3.3.5 Conclusions

We have demonstrated that PEI can effectively bind and protect plasmid DNA for efficient gene transfer. The parameters for complexation between PEI and pDNA were optimized, to find the most suitable conditions that led to improved systems, in terms of encapsulation efficiency, zeta potential, and size. Polyplexes were formulated at different N/P ratios and characterized using agarose gel electrophoresis, DLS, and by measuring surface charge. As the overall charge ratio of the carriers increased, the carriers complexed pDNA more effectively. Furthermore, the PEI-pDNA complexes had smaller hydrodynamic diameters and larger zeta potentials as the N/P ratio increased. Using the knowledge between overall charge ratio and polyplex composition, polyplexes were formulated at various N/P ratios with GFP-encoding pDNA to investigate the ability of polyplexes to promote therapeutic gene expression. Fluorescence microscopy images revealed that lower charge ratios exhibited smaller levels of gene transfer. As the charge ratio of the polyplex increased, the transfection efficiency was seen to drastically improved. These findings can be explained by the fact that the smaller, more positively charged nanocarriers, corresponding to a higher N/P ratio can more readily be endocytosed and achieve endosomal escape through the proton sponge effect. Cellular trafficking experiments using pulse-chase transfection and fluorescence microscopy can be performed to unveil the specific transport mechanisms used by polyplexes at different N/P ratios to achieve therapeutic delivery. Although higher N/P ratio complexes were more efficient at delivering therapeutic cargo, prior work by the group showed that PEI-pDNA polyplexes at larger charger ratios exhibit significant levels of cytotoxicity. The cytotoxicity concerns limit translation of PEI-based vectors into *in vivo* applications; however, these complexes serve as a suitable vector for studies concerning nonviral *in vitro* gene delivery. Modifications to the PEI polymer could be explored to reduce toxicity while simultaneously improving gene transfer. This research work will enable researchers to access a full range of conditions that could be applied for PEI polyplex formulation as well as will enable them to predict the kind of properties concerning the encapsulation efficiency, zeta potential, mean diameter, polydispersity, cytotoxicity, and protein

expression that the systems can provide. Furthermore, it will allow for scientists to synthesize nanocarriers with certain characteristics to study the potential of PEI-based polyplexes for treatment of diseases and disorders that have been difficult to address by conventional methods such as cancer, chronic wounds, hemophilia, etc.

Chapter 4

EFFECT OF CELL MIGRATION ON PEI-pDNA POLYPLEX TRANSFECTION EFFICACY AND MECHANISM

4.1 Background and Motivation

4.1.1 Wound Healing

The Wound Healing Society states that wound is the result of "disruption of normal anatomic structure and function" and are classified as acute or chronic based on the progression of the wound healing process.[56] Skin wounds have a tremendous negative impact on healthcare systems and the economy worldwide. Overall, in the United States approximately 2% of the total population are estimated to be affected by chronic wounds,[57] a number that translates into huge financial expenditures. It was estimated that in developed countries, the expenditures associated with chronic wound management accounted for as much as 3% of total healthcare spending.[58] For instance, in the United States, the overall costs associated with chronic wounds is approximated to be 50 billion USD per year.[59] The situation is likely to be aggravated by low healing rates. In fact, it was reported that publicly available healing rates for skin wounds were significantly overestimated. In particular, the data from randomized-controlled studies provides an average healing rate of 40%, whereas the reported rate is usually greater than 90%.[60]

Nonhealing wounds are most frequently generated by endogenous mechanisms due to a predisposing condition which ultimately compromises dermal and epidermal tissue integrity. The formation of chronic wounds such as leg ulcers, foot ulcers, and pressure sores could be a consequence of impaired arterial supply or impaired venous drainage and metabolic diseases such as diabetes mellitus.[61] Chronic wound formation could also be the result of aging, obesity, smoking, poor nutrition, or immunosuppression associated with disease (e.g., AIDS) and drugs (e.g., chemotherapy or radiation therapy).[62] However, the formation of pressure or decubitus ulcers is caused by prolonged pressure on the skin, most commonly on skin that covers bony areas of the body, such as the heels, ankles, hips, and tailbone. In any case, the underlying

pathology is often responsible for the chronicity, and all heal slowly in an unpredictable manner.[63] The increasing prevalence of communicable and noncommunicable diseases along with poor lifestyle choices render strategies to improve chronic wound healing even more imperative.

Given the abundance of research on the regulation of genes in chronic and other wound healing disorders, nucleic acid approaches provide the most effective means of translating this knowledge into therapies that have large potential impact. Furthermore, recent advances in enhancing nucleic acid vector stability and in the manufacture of RNA and DNA constructs make such therapeutic approaches much more accessible with regard to cost, manufacturing feasibility, and product availability. The engineering of delivery systems that enable these therapeutics to reach the appropriate cells and enable controlled and appropriately staged release will yield exciting new treatments for chronic wounds and other healing disorders in the upcoming decade.

4.1.2 Phases of Wound Healing

The wound healing process consists of four phases: hemostasis, inflammation, proliferation and migration of cells, and tissue remodeling or resolution. Hemostasis begins immediately after the injury and involves vascular constriction and aggregation of platelets to form a fibrin clot, from where proinflammatory cytokines and growth factors such as transforming growth factor (TGF), epidermal growth factor (EGF), fibroblast growth factor (FGF), and platelet derived growth factor (PDGF) are released.[64] When inflammation begins neutrophils clear the area for invading microbes and cellular debris around the wound and macrophages clear the area for apoptotic cells. Macrophages also stimulate other cells to promote tissue regeneration, thereby playing a role in promoting the next stage of wound healing, the proliferation and migration of cells.[64] Both endothelial cells and fibroblasts are present in the reparative dermis of the skin.[64] Fibroblasts and endothelial cells are attracted by mediators produced by inflammatory cells in the wound, and the cells proliferate to expand and migrate

into the wounded area.[65] Within the wounded area fibroblasts produce various compounds including collagen, which is a major component of the skin extracellular matrix.[64] Skin fibroblasts can change their character; for example, in a wound they can change their actin gene expression and take on some contractile properties of smooth muscle cells and in this way help to pull together the etches of the wound. Such fibroblasts are called myofibroblasts.[65]

Fibroblasts can be arrested in a specialized nondividing state called the G0 phase until they are triggered to proliferate by a growth factor or other extracellular signals. There are many proteins that act as mitogens, but PDGF is believed to have an important role in stimulating cell division during wound healing.[65] The fourth and last phase of wound healing is scar formation and remodeling of the tissue. An important part of this phase is the extracellular matrix attaining the architecture of normal tissue. Therefore, fibroblasts also have a role in this phase of wound healing.[65]

4.1.3 Nonviral Delivery Using Polymeric Nanoparticles For Wound Healing

Despite the past few decades of research, few new options have become clinically available to treat chronic wounds. New strategies are needed, and nonviral delivery of therapeutic nucleic acids may serves as a viable approach for promoting the healing of chronic wounds by controlling inflammation, extracellular matrix degradation, cell motility, angiogenesis, epithelialization, and oxidative stress. Nonviral approaches are less or nonimmunogenic, can incorporate larger payloads, are easier to manufacture, and lack the safety issues of viruses since they are nonintegrating. They also tend to be more modular and enable controlled release of the therapeutic cargo through a drug delivery system. A wide array of preclinical approaches to modulate wound healing have been investigated, including delivery of siRNA, plasmid DNA, anti-miRNA oligonucleotides, miRNA mimics, and antisense oligonucleotides.[66] For each of these approaches, different synthetic materials have been used, including dendrimers, lipid nanoparticles, polymeric micelles, polymer polyplexes, metal

nanoparticles, hydrogels. Combinations of these materials have been used as well to leverage the unique properties that each provides.

4.1.3.1 Delivery of Therapeutic Plasmids using PEI-based Delivery Strategies

To date, most *in vitro* delivery of therapeutic nucleic acids has been performed with cationic lipids, which are amphiphiles with a polycationic head group and hydrophobic tail groups. While cationic lipids were initially thought to be too toxic for *in vivo* application, certain lipids have been developed for safe low-dose usage in vivo.[67] The first siRNA therapy to gain FDA approval, Patisiran, is delivered with a lipid nanoparticle targeted to the liver.[68] However, polymer-based delivery systems have also been used for tissue repair or regeneration since they can be readily modified for various purposes. 25 kDa branched PEI is the most common cationic polymer employed in nonviral vectors for wound healing since it has a significantly higher gene transfer efficiency than linear PEI and other cationic polymers. Elangovan et al. utilized collagen scaffolds to deliver PEI-pDNA [encoding platelet derived growth factor-B (PDGF-B)] complexes in an attempt to optimize parameters of the polyplexes for the best balance between transfection efficiency and cytotoxicity.[69] The PEI-pDNA complexes achieved a high transfection efficiency at the optimal N/P ratio of 10. Then, they applied the gene-activated scaffolds onto calvarial defects in Fisher 344 rats. The pPDGFB-activated scaffold favored cellular attachment and promoted cellular proliferation *in vitro*; it also promoted osteogenesis and demonstrated superior tissue regeneration efficacy in calvarial defects in rats when compared to the empty defect and empty scaffold groups. Peng et al. encapsulated their plasmid DNA encoding VEGF in a β-cyclodextrin-graft-PEI nanoparticle and then loaded these nanoparticles into an epidermal stem cell-coated gelatin matrix, which could be applied directly to the wound as a dressing.[70] Ban et al. recently demonstrated intradermal injection of a mimic for the anti-inflammatory miRNA, miR-497, which has been implicated in modulating the NF-κB inflammatory signaling cascade. They delivered their miRNA mimic by injecting polyplexes of

the nucleic acid with PEI into diabetic ulcers.[71] The promising results from these studies and ongoing work has stimulated interest in developing PEI vectors to treat chronic wounds.

4.1.3.2 Wound Environment Delivery Challenges

Despite the many advantages of nonviral delivery, there are also unique challenges posed by the wound environment, six of which are highlighted by Whittam et al.[72] Delivered therapeutics are exposed to the external environment, making it challenging to retain them with dressing changes, debridement, or normal movement. High levels of reactive oxygen species can damage the therapeutics, their delivery vehicles, or the desired target cells. Additionally, high concentrations of proteases in the wound area can degrade the nonviral delivery system and reduce the amount of endogenous growth factors. For example, matrix metalloproteinases, a group of calcium-dependent zinc-containing enzymes that are involved in the degradation of extracellular matrix, are overexpressed in chronic wounds, increasing the difficulty of chronic wound treatment.[73] Poor perfusion around the wound lowers the cell viability and leads to swelling, which significantly reduces the transport kinetics of nonviral delivery systems and the local acidity. Infected or dead tissues will also impact which cells uptake the delivered therapeutic.[72]

4.2 Research Aims 2 and 3 - Develop and utilize a simple *in vitro* wound model to characterize the effect of cell migration and expression of migratory signals on polyethylenimine/pDNA polyplex transfection

Cell migration is a multistep process that is essential for diverse life functions in multicellular and single-celled organisms and includes both collective and individual cell movements across extracellular spaces or through tissues. In normal physiological processes, migration enables morphogenesis, immunity, and tissue repair.[74] During wound healing, cells proliferate and migrate into the wounded area, with the migration phase being the bottleneck in the healing process. To model the wound healing process *in vitro*, a confluent cell monolayer can be deliberately destroyed, thus creating a cell-free region available for cells to bridge and repair.

The migration of cells into the formerly cell-populated area can then be documented and analyzed. Many two-dimensional (2D) wound healing assays have been developed and used to study the molecular mechanisms of wound repair, as well as in the investigation of potential therapeutics and treatments for improved healing. The most common 2D wound healing assay is the "scratch assay" which introduces a wound mechanically to a confluent cell layer by scratching. Additional methods for cell injury include thermal, electrical, and optical wounding.[75] The basic steps of the scratch assay involve creation of the scratch on monolayer cells, capture of images at the beginning and regular intervals during cell migration close to the scratch, and comparison of the images to study effects of treatments. One of the major advantages of this simple method is that it mimics to some degree migration of cells *in vivo*. Furthermore, the patterns of migration either as loosely connected populations in the case for fibroblasts, or as sheets of cells for epithelial and endothelial cells also mimic the behavior of these cells during migration *in vivo*.

The wound healing assay is a convenient and economical method to investigate collective cell migration under different experimental conditions. The assay has been used to investigate the effects of the cell-matrix and cell-cell interaction on cell migration and combined with transfection to determine the effect of the expression of exogenous genes or downregulation of endogenous genes on the migration of individual cells. However, the assay combined with transfection has yet to focus on how the migration of cells affects the efficacy and mechanism of polymeric nanoparticle carriers. Understanding these effects could facilitate the development of therapeutic interventions for a wide range of diseases, including chronic wounds.

4.3 Results and Discussion

4.3.1 *In-vitro* Wound Model Development

To test the effects of cell migration on polyplex transfection, an *in vitro* wound model needed to first be developed that could be combined with the transfection procedure employed in

the prior chapter. Since the *in vitro* scratch assay using mechanical wounding was a simple, economical method to model cell migration *in vivo*, and was well documented in literature, this protocol was chosen for the following experiments. Mechanical wounding of a cell monolayer to simulate a wound has been done with a variety of sharp objects such as pipette tips[76], cell scrapers[77], metallic microindenters[78], and toothpicks.[79] Additionally, for procedures using pipette tips, different sized tips were used. To study the effects of cell migration on transfection, the scratch needed to be large enough to allow for cells to migrate to close the scratch but not so large that a majority of the scratch would not be closed after 24 hours. To determine which size pipette tip would best result in this outcome, an *in vitro* scratch assay procedure adapted from Rodriguez et al.[80] was followed using a 200 μL and 1000 μL pipette tip. Briefly, NIH/3T3 cells were seeded in 12-well plates (40×10^3 cells/well) and allowed to grow to a confluent monolayer. After replacing the growth medium with PBS, a linear scratch was made with either a 200 μL or 1000 μL pipette tip. The PBS was replaced with growth medium, and the cells were allowed to incubate for 24 hours.

The closure of the scratch was observed using a phase contrast microscope at 0 and 24 hours after wounding, which are displayed in Figures 4-1 and 4-2. To quantify the closure of the scratch**,** the difference between wound width at time 0 and time 24 hours was determined. Each well was marked below the plate surface by drawing a horizontal line, to allow identification of the same scratch area in order to take consistent pictures. Wound width was measured using ImageJ software (National Institutes of Health, Bethesda, MD, USA). The migration rate for each well was calculated as percentage of scratch closure on an initial width basis according to the equation found in Chapter 2. The average percent of wound healing after 24 hours for each pipette tip size is plotted in Figure 4-3. The data are presented as means ± SD of three independent scratches. Cells wounded with the smaller pipette tip healed nearly twice as much as cells scratched with the larger 1000 μL, healing 51.2% of the generated wound compared to only 25.7%.

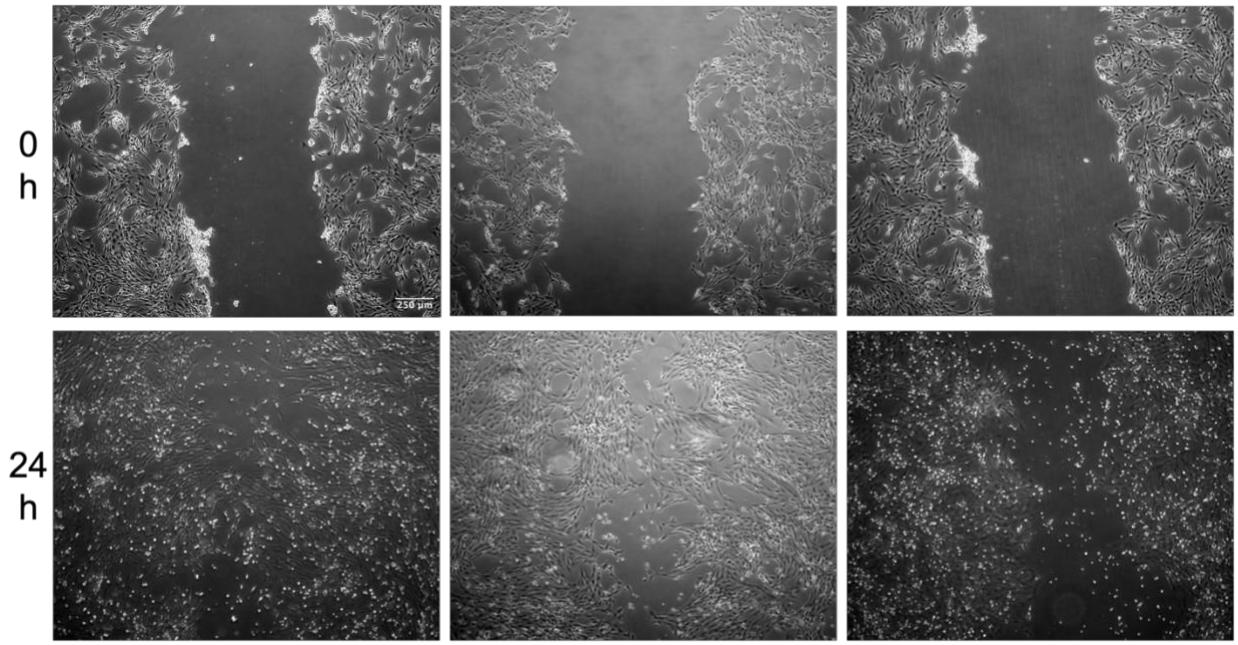

Figure 4-1. Representative phase contrast micrographs of NIH/3T3 cells scratched with a 200 µL pipette tip for 0 and 24 hours. The scale bar (shown in top left image) = 250 µm.

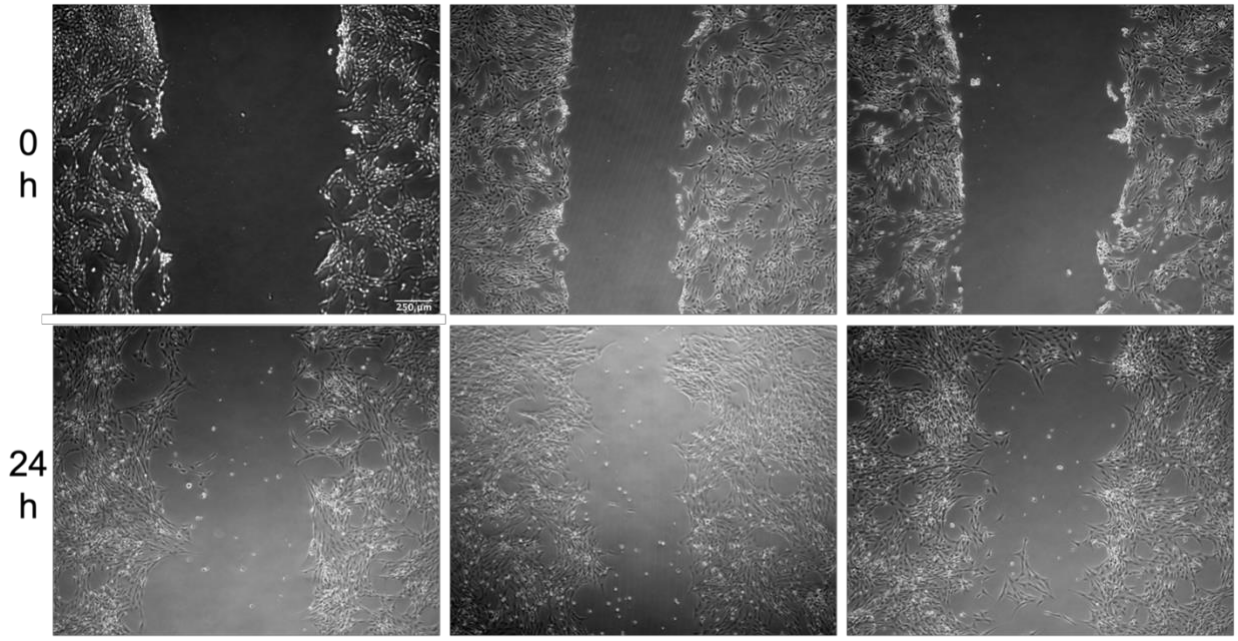

Figure 4-2. Representative phase contrast micrographs of NIH/3T3 cells scratched with a 1000 µL pipette tip for 0 and 24 hours. The scale bar (shown in top left image) = 250 µm.

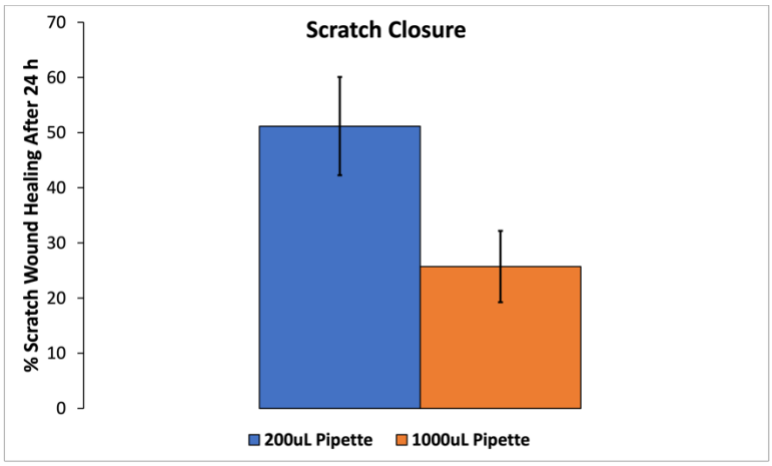

Figure 4-3. Average scratch wound healing 24 hours following mechanical wounding with a 200 μL (blue) and 1000 μL (orange) pipette tip. Results are shown as the mean ± standard deviation of data obtained from three independent measurements.

4.3.2 Cell Transfection Using *In-vitro* Wound Model

Since the standard transfection procedure requires analyses after 24 or 48 hours, based on the migration rates displayed in Figure 4-3, a 200 μL was chosen as the wounding tool for all scratch assay experiments. The greater amount of wound healing with the smaller pipette tip would ensure that ample migration occurs during the transfection process and provide more migratory cells to be analyzed compared to non-migrating cells. Previous studies using nanoparticles to deliver siRNA or pDNA treated cell monolayers before wounding.[81] Additionally, protocols for combining transfection with *in vitro* scratch assays also transfected cells prior to scratching.[76] However, performing gene transfection before scratching does not allow for isolation of the effect of cell migration or migratory signals on transfection. Thus, the protocols outlined in literature were adapted to transfect the cells after wounding the cell monolayer rather than before. Following mechanical wounding, rather than replacing PBS with growth media, 0.8 mL of Opti-MEM® and 0.2 mL of polyplex solution were added dropwise throughout each well. Additionally, for these transfection experiments, four scratched wells were not transfected, and four non-scratched wells were transfected to serve as controls. The experimental setup for these wound scratch assays with transfection can be seen in Figure 4-4.

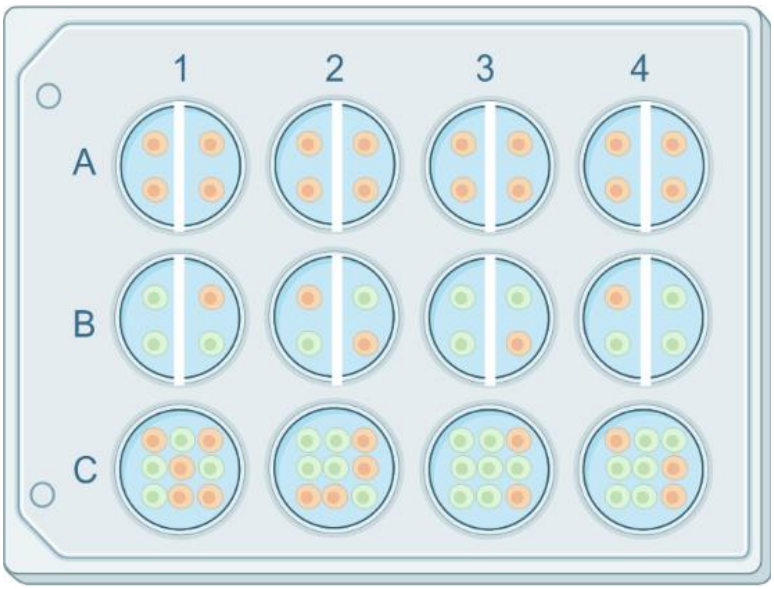

Figure 4-4. Schematic of 12-well plate for wound scratch assays with transfection. Cells scratched but not transfected (Row A), cells scratched and transfected (Row B), and cells transfected but not scratched (Row C) were analyzed for each experiment.

Based on the previous studies from Chapter 3, for optimal transfection efficiency, PEI-pDNA polyplexes were formulated at an N/P ratio of 10 for the transfections with the wound scratch assays. After acquiring phase-contrast images, such as those seen in Figure 4-5, the cells were incubated for hours, the transfection medium was removed, and 1 mL of fresh DMEM was added to the cells. The cells were then incubated for 48 hours, and phase-contrast images of each scratch were acquired after 24 and 48 hours. Examples of these images of a well from one experiment can be seen in Figure 4-6.

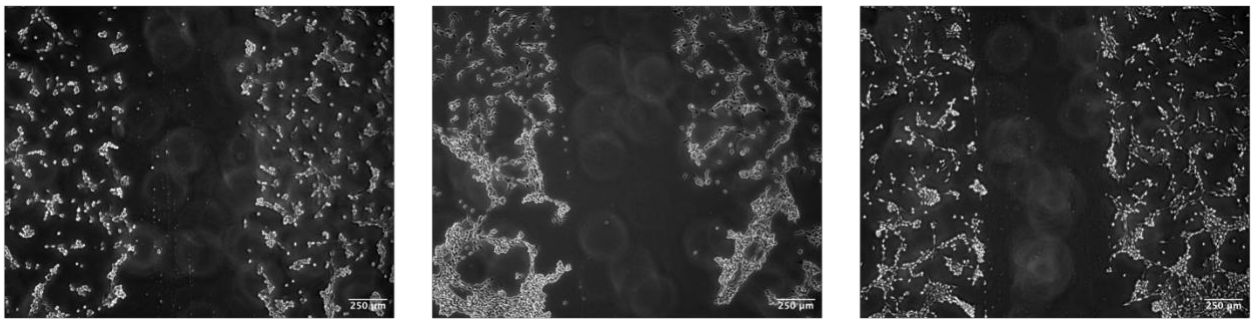

Figure 4-5. Three representative phase contrast images of mechanically wounded NIH/3T3 cells following immediately following polyplex dosing. The scale bar (shown in each image) = 250 µm.

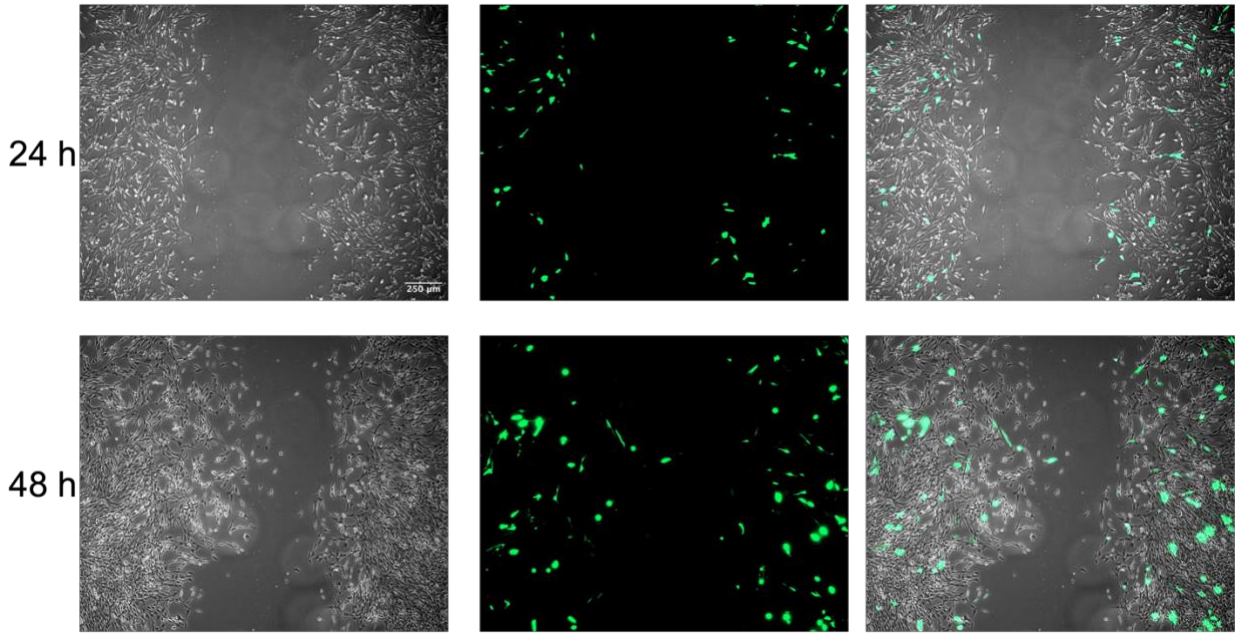

Figure 4-6. Transfection efficiencies of PEI-pDNA polyplexes 24 hours post-transfection and wounding. Phase contrast microscopy (left), fluorescence microscopy (middle), and overlay (right) images of one well following transfection with N/P 10 polyplexes. The scale bar (shown in top left image) = 250 µm.

Transfection analyses were carried out using in ImageJ to determine whether migratory cells more readily endocytosed polyplexes and expressed the plasmid DNA encoding GFP. Flow cytometry could not be used to measure transfection efficiencies since the technique can only provide transfection efficiencies for an entire well. Therefore, a flow cytometer could not measure successful transfection of only the migratory cells. Data from four transfected wells after 24 hours from three independent experiments were utilized for the analyses. Transfection efficiencies for the wound scratch assays after 48 hours were not measured since cell proliferation becomes a confounding variable, which would not allow the assays to specifically assess the effect of migration on transfection. For longer term transfection studies (> 24 hours) aiming to study the effects of cell migration, mitosis inhibitors such as mitomycin C treatment could be applied to inhibit cell proliferation.

Since time-lapse microscopy with live cell imaging was not utilized for cell tracking, to differentiate between the areas containing migratory and non-migratory cells, the scratch widths

of the time 0 and time 24 images for each well were compared. A representative well with the corresponding areas labeled can be visualized in Figure 4-7.

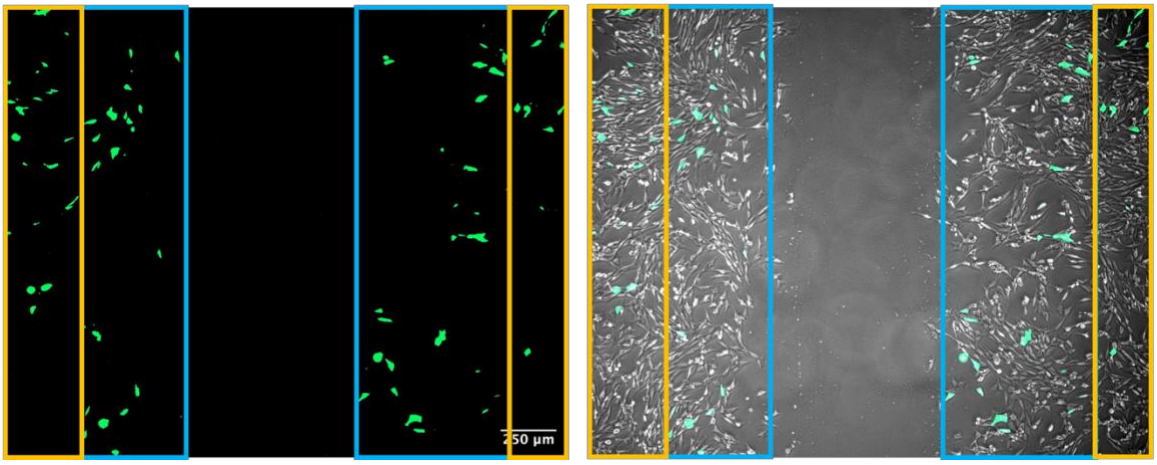

Figure 4-7. Representative wounded well with migratory area (blue) and non-migratory area (orange) indicated by the region within the rectangles. The scale bar (shown in the left image) = 250 µm.

To quantify the transfection efficiency of migratory cells compared to non-migratory cells, the integrated fluorescence intensity of each set of cells after the 24 hour incubation period was measured using ImageJ. The average integrated fluorescence intensity for each set of cells was calculated using six independent samples and the data was normalized with respect to the non-migratory integrated fluorescence intensity.

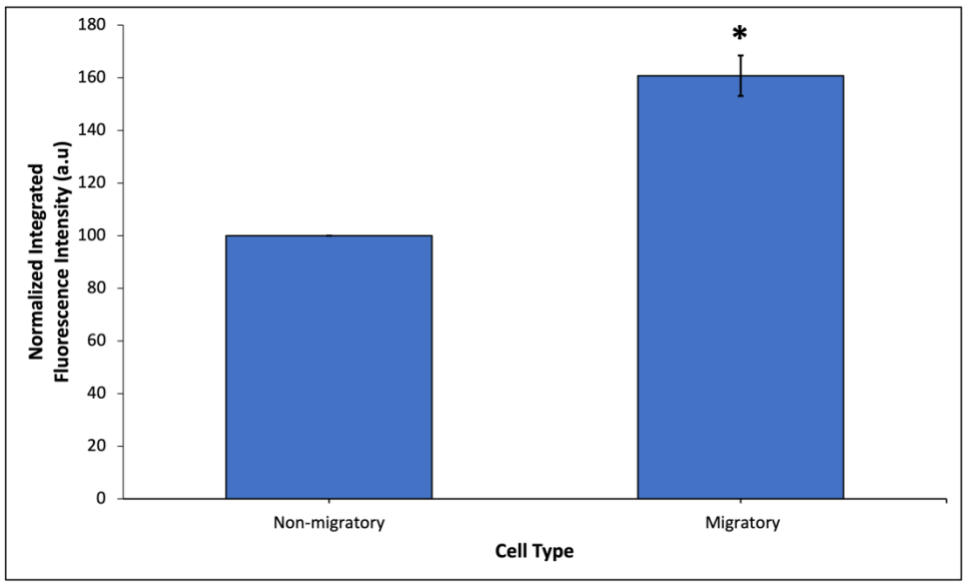

Figure 4-8. Transfection efficiencies of N/P 10 polyplexes in migrating and non-migrating cells. Integrated fluorescence was calculated using the area of interest and the mean intensity of the cells in the respective area, using ImageJ software. The integrated fluorescence intensity was normalized with respect to the non-migratory cells. Results are shown as the mean ± standard deviation of data obtained from six independent samples; * indicates a statistically significant difference between the migratory and non-migratory values ($p < 0.05$).

As shown in Figure 4-8, transfection occurred more readily in cells that were migrating to close the gap compared to cells that remained adherent to the plate and only underwent proliferation. The greater rates of transfection in migratory cells could be explained by the codependence that transfection and cell migration share on endocytic and endosomal trafficking. Originally, the rate of endocytosis had been proposed to be higher at the cell's trailing end to achieve polarized bulk recycling of membrane and/or adhesion molecules to the leading-edge during migration.[83] However, it is now accepted that endocytosis at the leading edge is crucial for cell migration by spatially restricting localization of signaling receptors and occurs at an increased rate. The localization and dynamics of clathrin-mediated endocytosis, caveolin-mediation endocytosis, and clathrin-independent pathways during cell migration have been investigated, with the clathrin pathway being the best-understood to date.[84]

Endocytic trafficking contributes at multiple steps for the regulation of the different processes required for cell migration. First, binding of scavenge receptors to secreted

chemokines and the subsequent endocytosis of the receptor-ligand complexes contributes to the development of chemotactic gradients. Chemokine receptor internalization and intracellular trafficking are key for efficiency and regulation of cell migration by keeping chemotactic receptors in place. Chemokine binding enhances steady-state internalization and endosomal trafficking of the receptor. The major route of chemokine receptor internalization is through clathrin mediated endocytosis; however, chemokine receptors have also been shown to utilize caveolar-dependent pathways.[85,86] These receptors eventually proceed to late endosomes/lysosomes through clathrin-coated vesicles where they are either degraded or dissociated from their ligand and enter the recycling compartment to traffic back to the plasma membrane.[85] Small GTPases of the Rab family are responsible for the regulation of the intracellular trafficking steps, such as those seen in Figure 4-9, for both internalized nanocarriers and chemokine receptors.[83] Border cell migration also requires endocytosis to counteract delocalization of guidance signaling by lateral diffusion of guidance receptors and to regulate trafficking of receptor tyrosine kinases (RTKs) through the endosomal system for their recycling to a specific region of the plasma membrane. Finally, endocytic pathways are needed for regulating downstream signaling and actin regulatory components.

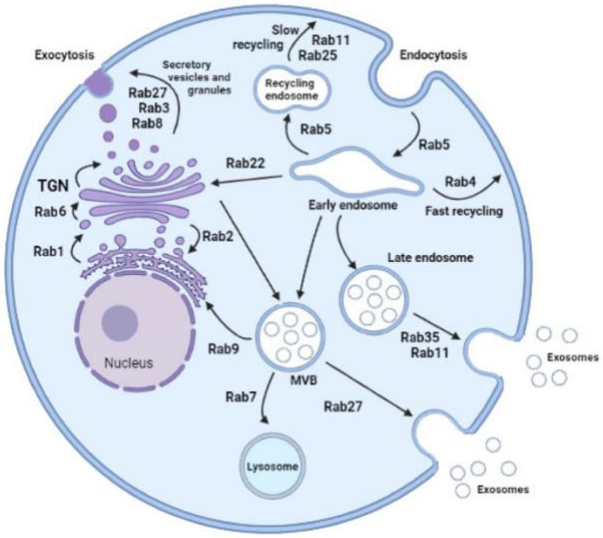

Figure 4-9. Rab proteins-mediated intracellular vesicular transport. Highlighted Rab family proteins that play key roles in regulating cellular membrane trafficking including endocytosis, exocytosis, exosome secretion, and vesicles delivery between organelles. Small Rab GTPases play key roles regulating cellular vesicular trafficking including endocytosis, exocytosis, exosome secretion, and intracellular vesicles delivery.[87]

With this in context, since PEI engineered nanocarriers also utilize clathrin- and caveolae-mediated endocytic mechanisms to achieve successful transfection, the increased rate of endocytosis in migratory cells could enable polyplexes to be internalized more readily. This hypothesis is supported by studies that have shown that PEI polyplexes utilize endocytic and trafficking pathways regulated by Rab proteins, which also regulate cell migration.[88,89] Rab5, considered as the first Rab GTPase encountered during both clathrin-mediated and caveolae-mediated endocytosis,[90] controls endocytosis and early endosome fusion for both growth factor receptors and engineering nanocarriers. It is speculated that there is increased trafficking through and colocalization of polyplexes with Rab5-mediated pathways for polyplexes in migrating cells compared to non-migrating cells due to the increased recycling of growth factor receptors via these pathways which can be visualized in Figure 4-10. Polyplexes could then traffic through further endolysosomal pathways and utilize the proton sponge effect to escape endosomes and deliver their therapeutic cargo to the intracellular target.

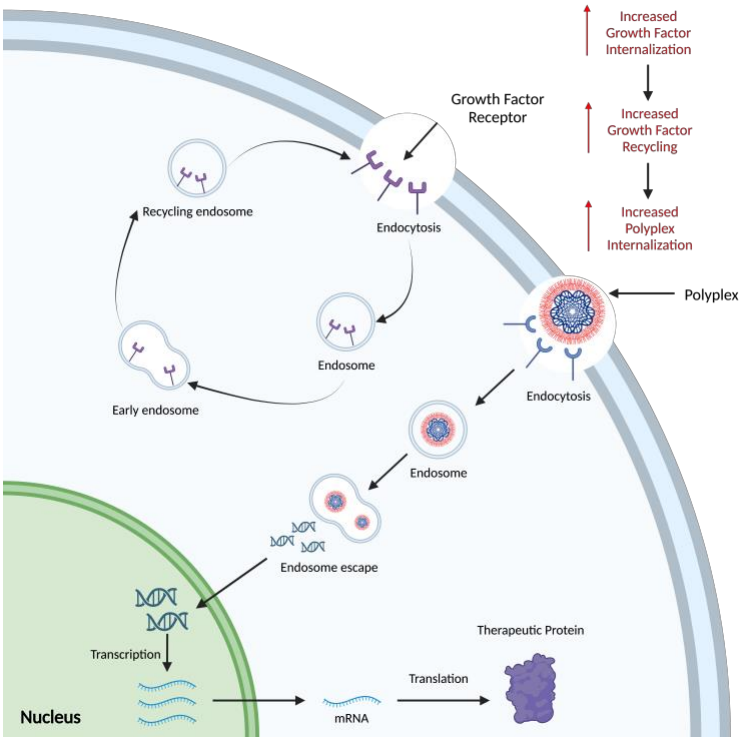

Figure 4-10. Suggested hypothesis for increased polyplex transfection in migrating cells due to increased trafficking through Rab5-mediated pathway. Rab5, which is localized to early endosomes mediates endocytosis and endosome fusion of vesicles.

Another important observation observed was the fact the polyplex transfection did not impede the rate of cell migration. Figure 4-11 displays mechanically wounded NIH/3T3 cells that were transfected and not transfected at certain time periods following scratching. Even though transfection occurred more readily in migrating cells, these cells still migrated at approximately the same rate to close the wound. It is hypothesized that growth factor receptors and polyplexes traffic through different Rab-linked endocytic pathways following early endosome fusion, thereby not impeding the rate at which polyplexes can reach the target site. A majority of growth factor receptors in migrating cells are likely being recycled to the cell surface slowly through Rab11-meditaed pathways, or directly through Rab4-controlled pathways. Some receptors may be moved to the lysosome for degradation via pathways regulated by Rab7. On the other hand, a lower fraction of polyplexes are likely being trafficked through recycling endosomes controlled by Rab11 to the cell surface and are escaping early or late endosomes

associated with Rab5 and Rab7, respectively. Thus, transfection with therapeutic pDNA could be used to enhance the rate of wound healing without the delivery vector or process combating the therapeutic goal.

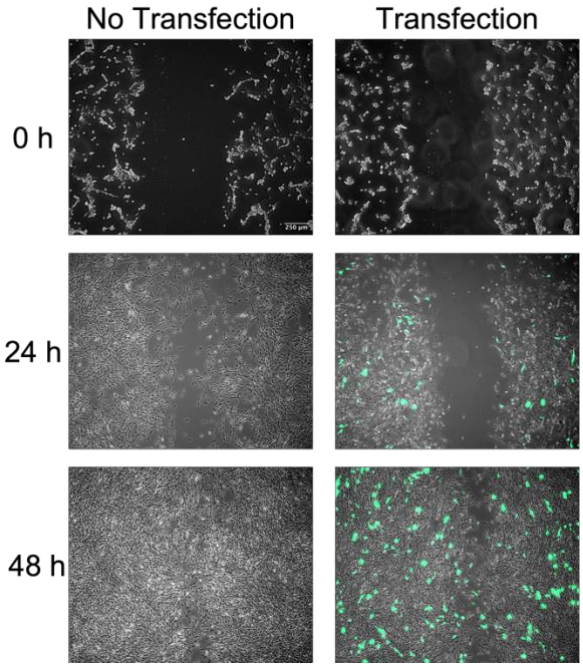

Figure 4-11. Representative phase contrast images of scratched NIH/3T3 cells without transfection (left column) and overlap images of scratched NIH/3T3 cells that were transfected (right column) 0, 24, and 48 hours after wounding. The scale bar (shown in top left image) = 250 μm.

4.3.3 Effect of Serum Supplementation on Cell Transfection

Cell migration is influenced by growth factors like PDGF and EGF that bind to their respective growth factor receptors. For example, cell migration begins with generation of a chemotactic gradient. Migrating cells must sense the chemotactic cues using chemotactic and growth factor receptors that induce intracellular signaling cascades.[84] Regulation of chemotactic and growth factor receptors through endocytic trafficking modulates the responsive of cells to these chemotactic cues. Thus, we sought to observe how the concentration of growth factors and cytokines in the cell culture media, or the extracellular environment, affects transfection of migrating cells. To alter the level of growth factors and cytokines in the extracellular environment, DMEM was supplemented with only 0.2 vol% FBS rather than 10%. In the 1950s,

when FBS was introduced in cell culture, it was thought that FBS would only stimulate the cell growth.[91] Later it was identified that FBS has essential components required for cell attachment, migration and maintenance, including growth factors and cytokines such as PDGF and EGF.[92] Based on role of growth factors and cytokines in regulating cell migration, we hypothesized that transfection efficiency of migratory cells would be lower using 0.2 vol% FBS compared to cells transfected using 10 vol% FBS. Using the *in-vitro* scratch assay, a confluent monolayer of NIH/3T3 was scratched and transfected with N/P 10 polyplexes following the protocol outline in Chapter 2. For transfection with reduced serum, the growth medium following polyplex incubation was replaced with DMEM supplemented with 0.2% FBS by volume rather than 10% and the cells were allowed to incubate for 24 hours. Phase contrast and fluorescence microscopy images were taken, which are displayed in Figure 4-12.

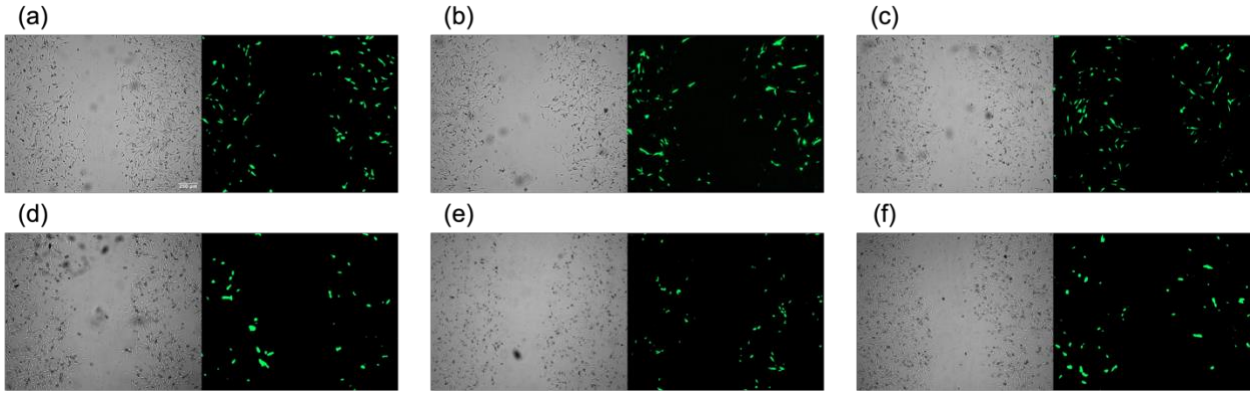

Figure 4-12. Transfection efficiencies of PEI-based polyplexes with different FBS concentrations. Data analyses were performed 24 h post transfection. Phase contrast microscopy (left) and fluorescence microscopy (right) images of scratched NIH/3T3 cells transfected using DMEM supplemented with 10 vol% FBS (a-c) and 0.2 vol% FBS (d-f). The scale bar (shown in panel a) = 250 μm.

The transfection efficiency of migratory cells compared to non-migratory cells was quantified in the same manner as before, and the results are plotted in Figure 4-13. Transfection using 10 vol% FBS agreed with findings previously observed. DMEM supplemented with 10 vol% FBS resulted in migratory cells being transfected more readily compared to non-migratory cells, with the transfection efficiency of cells migrating to close the wound being about 25%

greater. However, when cells were transfected with 0.2 vol% FBS, the transfection of migrating cells compared to non-migrating cells was significantly reduced. The transfection efficiency of migrating cells with reduced serum was about 60% of the efficiency of non-migrating cells. When comparing the migratory transfection efficiencies with respect to the non-migratory for each level of FBS, when normalized to the transfection of non-migrating cells, the transfection efficacy of migratory cells in 0.2 vol% FBS was nearly half of the efficiency in 10 vol% FBS. Additionally, Figure 4-11 reveals that the overall transfection efficiency of the PEI-based polyplexes was lower using 0.2 vol% FBS, which is likely the result of reduced cell proliferation during the 24 hours following transfection. Numerous studies have shown that gene delivery occurs more readily in diving cells, which is the result of increased nuclear access when the nuclear envelope disassembles during mitosis.[93,94]

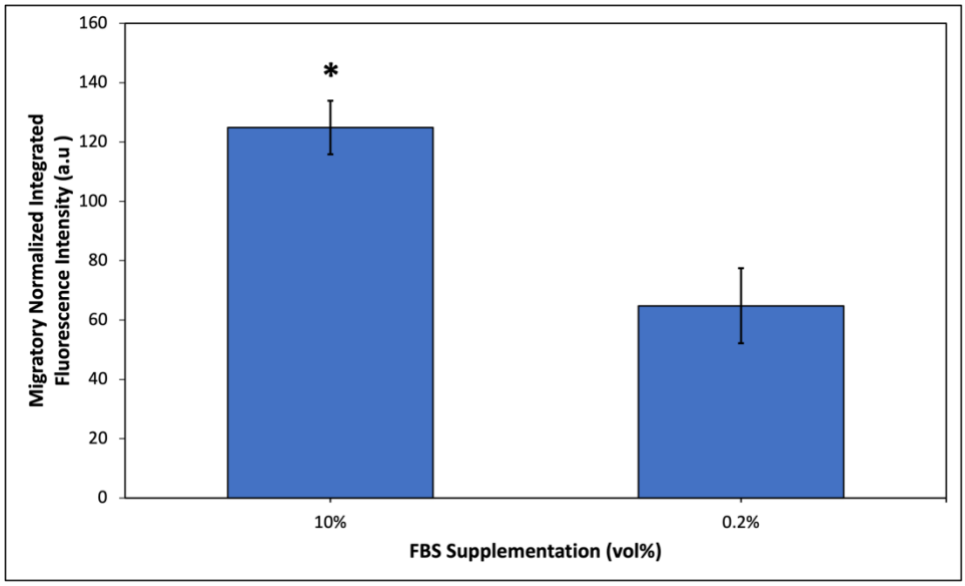

Figure 4-13. Transfection efficiencies of N/P 10 polyplexes in migrating cells with varying FBS supplementation. Integrated fluorescence was calculated using the area of interest and the mean intensity of the cells in the respective area, using ImageJ software. The integrated fluorescence intensity was normalized to the non-migratory cells for each of the respective FBS supplementations. Results are shown as the mean ± standard deviation of data obtained from six independent samples; * indicates a statistically significant difference between the 10 vol% and 0.2 vol% ($p < 0.05$).

The lower transfection of migrating cells using 0.2 vol% FBS is likely the result of a reduced internalization and trafficking of chemokine and growth factor receptors. Endocytosis is necessary to maintain RTKs and thereby guidance signaling spatially confined to the leading edge of the migrating cells to enable their polarization and directed migration. Additionally, as previously mentioned, endocytosis is also needed to regulate the trafficking of RTKs through the endosomal system for their recycling to a specific region of the plasma membrane. The small GTPases Rab5 and Rab11, which regulate early endosomal and slow recycling endosomal transport, were shown to be crucial for the polarization of guidance signaling during border cell migration.[95] In the mammalian system cell migration was shown to be dependent on RTK endocytosis. For example, an intracellular signaling pathway for PDGFRβ was discovered by which the Rac1 GEF DOCK4 and the GTPase dynamin2 control NIH3T3 cell migration in response to PDGF.[96] PDGFRβ becomes tyrosine phosphorylated upon ligand binding, enabling its interaction with the adaptor protein Grb2 which recruits DOCK4 and dynamin2 resulting in receptor endocytosis and Rac activation. The same study showed that blocking RTK endocytosis in NIH3T3 fibroblasts impaired migration.[96] With lower levels of growth factors such as PDGF in the cell culture medium, endocytosis and recycling of growth factor receptors regulated by Rab GTPases would be reduced. This reduction could indirectly affect polyplex transfection since aforementioned, clathrin- and caveolae-mediated endocytosis as well as endosomal escape are regulated by Rab GTPases. There would likely be decreased trafficking of growth factor receptors and polyplexes through Rab5-mediated pathways, leading to lower transfection efficiency. Since border cell recruitment is necessary for tissue regeneration, high transfection of these cells is desirable. The border cells can act as local *in vivo* bioreactors, generating therapeutic proteins that enhance tissue repair and regeneration. Thus, future strategies are needed to recruit external cells and have them migrate towards PEI/DNA complexes, where they can be transfected and help in tissue repair.

Chapter 5

CONCLUSIONS

The field of polymer-based gene delivery has the potential to make advancements towards personalized medicine and treatment of chronic wounds. The work herein addresses three research aims to optimize the formulation of PEI/pDNA polyplexes and characterize the effects of cell migration and migratory signals on their efficacy *in vitro*. The aims are as follows:

1) Optimize the formulation of polyethylenimine polyplex systems for efficient gene delivery
2) Develop a simple *in vitro* wound model for studying cell migration during gene delivery
3) Characterize the effect of cell migration and expression of migratory signals on polyethylenimine polyplex transfection

Towards Aim 1, it was demonstrated that using larger amounts of PEI, corresponding to a larger N/P ratio, decreased polyplex size, increased surface charge, and improved complexation of pDNA. These more positively charged, smaller complexes resulted in higher gene expression of GFP-encoded pDNA, but simultaneously decreased the cell viability, illustrating a tradeoff between PEI-based polyplex transfection efficiency and cytotoxicity. These trends were observed through formulation and characterization of PEI-based polyplexes up to an N/P ratio of 10, from which it was concluded that N/P 10 was the optimal N/P ratio for transfection of NIH/3T3 cells using PEI-pDNA polyplexes. However, the optimal N/P ratio to achieve the most gene expression varies by cell line since cellular uptake rate and unpacking within endolysosomal compartments can differ.[97] Once the optimal formulation conditions were determined, a simple *in-vitro* wound model was developed that could be used to study the effects of cell migration and migratory signals associated with wound healing on PEI-pDNA polyplex transfection, which addresses Aim 2. In looking at Aim 3, it was found that border cells migrating during the wound healing process were preferentially transfected compared to cells not

involved in wound closure. Additionally, when the concentration of growth factors and cytokines in the extracellular environment was reduced, the transfection of migratory cells was reduced.

Chapter 6

FUTURE WORK

There are numerous possible paths for future developments with PEI-pDNA gene delivery systems to treat chronic wounds. Some possibilities include reducing the cytotoxicity while enhancing the transfection efficiency of PEI-based polyplexes and improving the understanding of the mechanisms utilized by these vectors to gain access to and navigate through the intracellular space to achieve successful gene delivery. Additionally, creating an *in-vitro* wound model that better emulates the *in vivo* environment and enables consistency between each experiment, as well as understanding the concurrent roles of different trafficking proteins in both the cell migration and transfection processes can be explored.

6.1 Reduction of PEI-Mediated Cytotoxicity

The work herein aims to advance the knowledge of PEI-based polyplexes for nucleic acid delivery to treat chronic wounds, advancing the rate of at which these vectors reach clinical implementation. However, the cytotoxic complications associated with cationic polymers have generated a negative trait for their possible application in gene therapy, and serious safety concerns have impeded clinical applications of PEI-based gene therapeutics. In addition, PEI-mediated cytotoxicity can antagonize transgene expression and, therefore, represents a limiting factor for high gene transfer activity. Accordingly, wide-ranging attempts with advanced polymer technologies and chemical engineering have been comprehensively utilized to design safer polymer derivatives. The most promising approaches used to improve PEI transfection performance together with counteracting the toxic complications include biodegradable cross-linking of LMW PEI, statistical surface modification, and synthesis of block co-polymers.

PEIs of lower molecular weight are less cytotoxic, whereas PEIs of higher molecular weight are more cytotoxic but also more efficient transfection vectors.[36] Therefore, various studies have attempted to design PEI derivatives that are constructed from LMW PEIs that are crosslinked through biodegradable bonds to ensure rapid degradation upon internalization.

Depending on the chemical nature of the cross-linkage, biodegradation can occur in different cellular compartments and stages of the nucleic acid delivery pathway. Various approaches have been used to construct biodegradable PEI derivatives from LMW PEIs, including strategies applying different functional group linkages to interconnect the small PEIs constituting the degradable PEI derivative. For example, the first biodegradable ester-linked linear PEI constituted PEIs of 800 Da that were produced by using 1,3-butanediol diacrylate as the cross linking agent.[97] The cytotoxicity of this biodegradable PEI derivative was found to be lower, and the transfection efficiency was 9-fold higher compared with 25-kDa linear PEI. Ester linkages have also been used to prepare biodegradable branched PEIs that had up to 16-fold higher transfection efficiency in comparison with branched 25-kDa PEI.[98]

Different engineering strategies have been used for statistical surface modification of 25-kDA branched PEI. For example, it has been shown that the extent of 25-kDA branched PEI acetylation, and thereby the modification of surface charge, can reduce cytotoxicity and improve transfection efficiency, although excessive surface modification can eliminate gene transfer.[99] The lower cytotoxicity from this strategy occurs because the surface modifications decrease the positive charge of the polymers, which lowers the inherent ability of the polymers to disrupt biological membranes. More complex PEI derivatization, which does not reduce the surface charge based on chemical blockade but, rather, steric shielding, is represented by the synthesis of co-polymers with non-cationic hydrophilic segments such as polyethylene glycol (PEG). The PEG segments reduce the inherent ability of PEI to disrupt lipid bilayers, which, in turn, makes it less likely to irreversibly damage the plasma membrane and other cellular organelles, such as early endosomes or mitochondria. One or multiple of these strategies could be explored to lower the toxic effects of PEI and improve transfection in devoid of or with cell migration. For example, our research group has found that incorporation of histone H3 tail peptides in combination with PEI simultaneously reduces cytotoxicity and amplifies transfection efficiency.[43] The ability of these vectors to transfect migratory cells compared to standard PEI-

based polyplexes could be investigated as a more viable strategy for *in vivo* wound healing studies.

6.2 Cellular Uptake and Trafficking of PEI-based Polyplexes and Growth Factors

Cellular internalization and subsequent intracellular processing of polyplexes are key barriers to successful in vitro gene delivery. As shown in this work, PEI-based gene delivery vectors possess high gene transfection efficiency, which can be attributed to its unique ability to simultaneously overcome several key barriers to intracellular trafficking of the nanocarriers, including escape from endosomes, protection of DNA from degradation by endonucleases, nuclear entry, and DNA release and transcription. However, the exact mechanisms of how PEI orchestrated the sequence of the intracellular processes required for effective expression of the transgene was unexplored. Understanding these mechanisms could explain the findings in this work, including the higher transfection efficiency seen in migratory cells compared to non-migratory cells. While clathrin-mediated endocytosis is the most commonly cited endocytic uptake pathway for PEI-based polyplexes, various studies show that the caveolar uptake route is often a more efficient gene transfer pathway for many carriers.[100] Confocal microscopy, cellular fractionation, super resolution microscopy, and fluorescence correlation spectroscopy experiments are methods that could be carried out to parse out the endocytic and intracellular trafficking pathways utilized by the nanocarriers in this experiment.[88] These protocols would provide insight into the kinetics of successful delivery and allow for visualization of the polyplexes in the intracellular space. Furthermore, various endocytosis inhibition studies could be performed to support the results from the preceding experiments. Transfection efficiencies could be measured in the presence of endolysosomal agents such as chlorpromazine, which inhibits clathrin-mediated endocytosis by dissociating clathrin from the plasma membrane,[101] and genistein, which inhibits caveolae-mediated endocytosis by inhibiting tyrosine-phosphorylation of Cav1,[102] to delineate what mechanism polyplexes are predominantly using to deliver their genetic cargo.

These techniques could also be applied to study the endocytic trafficking of growth factors and chemokines during cell migration, which could reveal possible shared mechanisms for nanocarrier and growth factor endocytosis in migrating cells. Additionally, transfection experiments with Rab-labeled GFP could be done to study colocalization of PEI polyplexes with Rab-linked endolysosomal compartments, which would provide useful insight into transfection in migrating cells where Rab proteins are also needed to regulate the migration process. To determine whether the rate of growth factor internalization is correlated with the rate of polyplex endocytosis, cellular transfection could be done and measurement of EGFR internalization rates using ^{125}I-EGF assays could be performed using established protocols.[103] The transfection efficiency and EGF internalization rate could be measured to determine if a relationship exists between the two. To further probe this relationship, transfection and the assays could be performed in the presence of endocytic inhibitors to see if both variables are affected in the same manner.

6.3 *In vitro* Wound Model Improvements

The *in vitro* scratch assay employed in this study served as a cheap and easy method to study cell migration. While the simple model has its pros, it also has a number of disadvantages and limitations. Cell proliferation can contribute to wound closure, manual scratching leads to variation in the size and shapes of the scratches, cells can accumulate on the edges of the scratch, and it can be difficult to relocate exact wound sites at sequential time points. Furthermore, analyzing the progress using a light-field microscope to take images of the scratch at pre-determined time points, followed by an analysis of the closure of the gap in an image software is time consuming. These aspects of the model can make analyses a burden and reduce the accuracy of the results.

One reported method to inhibit cell proliferation is serum starvation preceding the scratch,[104] however, this methods cannot ensure that there is no proliferation. To completely eliminate proliferation, one can pre-treat the cells with mitomycin C,[105] an antibiotic that inhibits

DNA synthesis by forming a covalent bond with the DNA.[105] For the *in-vitro* scratch assay used with transfection of cells, removing proliferation would improve the analysis of migratory transfection since the cells that contributed to wound closure could have been only the result of migration. Serum-free media has been shown as an effective media for cell transfections,[106] thus, either serum starvation or mitomycin C treatment could be employed to improve the model. To overcome challenges with reproducibility and quantification with mechanical scratching, live-cell microscopy techniques can be used to track cell migration rather than taking images at pre-determined time points.[107] Rather than performing manual data acquisition and analysis, which is time-consuming, error-prone and is subjective depending on the individual researcher, automated image analysis software tools could be explored for quantification with wound assays. ImageJ, MATLAB®'s Image Processing Toolbox, MultiCellSeg, and TScratch are software packages that could be used for automatic data analysis, each having their own strengths and limitations.[108] The aforementioned methods could be applied to the current work to reduce the time needed to conduct each experiment and better quantify the level of migratory transfection compared to non-migratory transfection. Determination of the migrating cells for each experiment would be more precise, reducing the subjectivity in the data analysis.

REFERENCES

1. Stone D. Novel viral vector systems for gene therapy. Viruses 2010;2:1002-7.

2. Katare DP, Aeri V. Progress in gene therapy: A review. I.J.T.P.R 2010;1:33.

3. Culver K, Cornetta K, Morgan R, Morecki S, Aebersold P, Kasid A, et al. Lymphocytes as cellular vehicles for gene therapy in mouse and man. Proc Natl Acad Sci USA 1991;88:3155-9.

4. Blaese RM, Culver KW, Miller AD, Carter CS, Fleisher T, Clerici M, et al. T lymphocyte-directed gene therapy for ADA-SCID: Initial trial results after 4 years. Science 1995;270:475-80.

5. Gardlik R, Palffy R, Hodosy J, Lukacs J, Turna J, Celec P. Vectors and delivery systems in gene therapy. Med Sci Monit. 2005;11:110–21.

6. Lehrman, S. Virus treatment questioned after gene therapy death. Nature 401, 517-518 (1999).

7. Ponti, F.; Campolungo, M.; Melchiori, C.; Bono, N.; Candiani, G.J.C.; Lipids, P.O. Cationic lipids for gene delivery: Many players, one goal. Chem. Phys. Lipids 2021, 235, 105032.Al-Dosari MS, Gao X.

8. Bono, N.; Ponti, F.; Mantovani, D.; Candiani, G.J.P. Non-viral In Vitro gene delivery: It is now time to set the bar! Pharmaceutics 2020, 12, 183.

9. Uğurlu, Ö.; Barlas, F.B.; Evran, S.; Timur, S.J.P. The cell-penetrating YopM protein-functionalized quantum dot-plasmid DNA conjugate as a novel gene delivery vector. Plasmid 2020, 110, 102513.

10. Boussif O, Lezoualc'h F, Zanta MA, Mergny MD, Scherman D, Demeneix B, et al. A versatile vector for gene and oligonucleotide transfer into cells in culture and in vivo: polyethylenimine.

11. Akinc A, Thomas M, Klibanov AM, Langer R. Exploring polyethylenimine mediated DNA transfection and the proton sponge hypothesis. J Gene Med. 2005;7:657–63.

12. Behr JP. The proton sponge: A trick to enter cells the viruses did not exploit. Chimia 1997; 51: 34-6.

13. Kafil, Vala & Omidi, Yadollah. (2011). Cytotoxic Impacts of Linear and Branched Polyethylenimine Nanostructures in A431 Cells. BioImpacts : BI. 1. 23-30. 10.5681/bi.2011.004.

14. Khalil IA, Kogure K, Akita H, Harashima H. Uptake pathways and subsequent intracellular trafficking in nonviral gene delivery. Pharmacol Rev 2006;58: 32-45.

15. Doherty GJ, McMahon HT. Mechanisms of endocytosis. Palo Alto, Ann Rev Biochem 2009; pp. 857-902.

16. Takei K, Haucke V. Clathrin-mediated endocytosis: membrane factors pull the trigger. Trends Cell Biol 2001; 11: 385-91.

17. Popova, N. V., Deyev, I. E., & Petrenko, A. G. (2013). Clathrin-mediated endocytosis and adaptor proteins. Acta naturae, 5(3), 62–73.

18. McMahon HT, Boucrot E. Molecular mechanism and physiological functions of clathrin-mediated endocytosis. Nat Rev Mol Cell Biol 2011; 12: 517-33.

19. Maxfield FR, McGraw TE. Endocytic recycling. Nat Rev Mol Cell Biol 2004; 5: 121 32.

20. Empig CJ, Goldsmith MA. Association of the caveolar vesicular system with cellular entry by filoviruses. J Virol 2002; 76: 5266-70.

21. Pelkmans L, Kartenbeck J, Helenius A. Caveolar endocytosis of simian virus 40 reveals a new two-step vesicular-transport pathway to the ER. Nat Cell Biol 2001; 3: 473-83.

22. Kirkham M, Parton RG. Biochim Biophys Acta. 2005;1745:273.

23. Parton RG, Simons K. The multiple faces of caveolae. Nat Rev Molec Cell Biol 2007; 8: 185-94.

24. Ferrari A, Pellegrini V, Arcangeli C, et al. Caveolae-mediated internalization of extracellular HIV-1 TAT fusion proteins visualized in real time. Mol Ther 2003; 8: 284-94.

25. Le PU, Nabi IR. Distinct caveolae-mediated endocytic pathways target the Golgi apparatus and the endoplasmic reticulum. J Cell Sci 2003; 116: 1059-71.

26. Sahay G, Alakhova DY, Kabanov AV. Endocytosis of nanomedicines. J Control Release 2010; 145: 182-95.

27. McLendon PM, Fichter KM, Reineke TM. Poly(glycoamidoamine) vehicles promote pDNA uptake through multiple routes and efficient gene expression via caveolae-mediated endocytosis. Mol Pharm 2010; 7: 738-50.

28. Remy-Kristensen A, Clamme JP, Vuilleumier C, Kuhry JG, Mely Y. Role of endocytosis in the transfection of L929 fibroblasts by polyethylenimine/DNA complexes. Biochim Biophys Acta 2001, 1514, 21–32.

29. Suh J, An Y, Tang BC, et al. Real-time gene delivery vector tracking in the endo-lysosomal pathway of live cells. Microsc Res and Tech 2012; 75: 691-7.

30. Dean DA, Strong DD, Zimmer WE. Nuclear entry of nonviral vectors. Gene Ther. 2005;12:881–890. doi: 10.1038/sj.gt.3302534.

31. Jerzykiewicz, J., & Czogalla, A. (2021). Polyethyleneimine-Based Lipopolyplexes as Carriers in Anticancer Gene Therapies. Materials (Basel, Switzerland), 15(1), 179.

32. Teif V.B., Bohinc K. Condensed DNA: Condensing the concepts. Prog. Biophys. Mol. Biol. 2011;105:208–222. doi: 10.1016/j.pbiomolbio.2010.07.002.

33. Fu J., Schlenoff J.B. Driving Forces for Oppositely Charged Polyion Association in Aqueous Solutions: Enthalpic, Entropic, but Not Electrostatic. J. Am. Chem. Soc. 2016;138:980–990. doi: 10.1021/jacs.5b11878.

34. S. Choosakoonkriang, B. A. Lobo, G. S. Koe, J. G. Koe, C. R. Middaugh, J. Pharm. Sci., 2003, 92, 1710.

35. M. Ogris, P. Steinlein, M. Kursa, K. Mechtler, R. Kircheis, E. Wagner, Gene Ther., 1998, 5, 1425.

36. Kunath, K., von Harpe, A., Fischer, D., Petersen, H., Bickel, U., Voigt, K., and Kissel, T. (2003). Low-molecular-weight polyethylenimine as a non-viral vector for DNA delivery: comparison of physicochemical properties, transfection efficiency and in vivo distribution with high-molecular-weight polyethylenimine. J. Control. Release 89, 113–125.

37. P. Erbacher, T. Bettinger, P. Belguise Valladier, S. Zou, J. L. Coll, J. P. Behr, J. S. Remy, J. Gene Med., 1999, 1, 210.

38. M. Hanzlikova, P. Soininen, P. Lampela, P. T. Mannisto, A. Raasmaja, Plasmid, 2009, 61, 15.

39. J. Fahrmeir, M. Gunther, N. Tietze, E. Wagner, M. Ogris, J. Control. Release, 2007, 122, 236.

40. Adolph, E. J., Nelson, C. E., Werfel, T. A., Guo, R., Davidson, J. M., Guelcher, S. A., & Duvall, C. L. (2014). Enhanced Performance of Plasmid DNA Polyplexes Stabilized by a Combination of Core Hydrophobicity and Surface PEGylation. Journal of materials chemistry. B, 2(46), 8154–8164.

41. Shi, J., Choi, J. L., Chou, B., Johnson, R. N., Schellinger, J. G., & Pun, S. H. (2013). Effect of polyplex morphology on cellular uptake, intracellular trafficking, and transgene expression. ACS nano, 7(12), 10612–10620.

42. Valente, J. F. A., Pereira, P., Sousa, A., Queiroz, J. A., & Sousa, F. (2021). Effect of Plasmid DNA Size on Chitosan or Polyethyleneimine Polyplexes Formulation. Polymers, 13(5), 793.

43. Meghan J. Reilly, John D. Larsen, and Millicent O. Sullivan. Molecular Pharmaceutics. 2012. 9 (5), 1031-1040.

44. Ogris, M.; Steinlein, P.; Carotta, S.; Brunner, S.; Wagner, E. DNA/Polyethylenimine Transfection Particles: Influence of Ligands, Polymer Size, and PEGylation on Internalization and Gene Expression. AAPS PharmSci 2001, 3, 43−53.

45. Perevyazko, I.Y.; Bauer, M.; Pavlov, G.M.; Hoeppener, S.; Schubert, S.; Fischer, D.; Schubert, U.S. Polyelectrolyte complexes of DNA and linear PEI: Formation, composition and properties. Langmuir 2012, 28, 16167–16176.

46. Foroozandeh, P.; Aziz, A.A. Insight into Cellular Uptake and Intracellular Trafficking of Nanoparticles. Nanoscale. Res. Lett. 2018, 13, 339.

47. Haeri A., Alinaghian B., Daeihamed M., Dadashzadeh S. Preparation and characterization of stable nanoliposomal formulation of fluoxetine as a potential adjuvant therapy for drug-resistant tumors. Iran. J. Pharm. Res. 2014;13:3–14. doi: 10.22037/ijpr.2014.1453.

48. Xie, Q.; Xinyong, G.; Xianjin, C.; Yayu, W. PEI/DNA formation affects transient gene expression in suspension Chinese hamster ovary cells via a one-step transfection process. Cytotechnology 2013, 65, 263–271.

49. Medina-Kauwe, L. K., Xie, J., & Hamm-Alvarez, S. (2005). Intracellular trafficking of nonviral vectors. *Gene therapy*, *12*(24), 1734-1751.

50. S. M. Moghimi, P. Symonds, J. C. Murray, A. C. Hunter, G. Debska, A. Szewczyk, Mol. Ther., 2005, 11, 990.

51. H. Zhang, T. Xia, H. Meng, M. Xue, S. George, Z. Ji, X. Wang, R. Liu, M. Wang, B. France, ACS Nano, 2011, 5, 2756.

52. K. Kunath, A. von Harpe, H. Petersen, D. Fischer, K. Voigt, T. Kissel, U. Bickel, Pharm. Res., 2002, 19, 810.

53. P. Chollet, M. C. Favrot, A. Hurbin, J. Coll, J. Gene Med., 2002, 4, 84.

54. Godbey, W. T.; Wu, K. K.; Mikos, A. G. Poly(ethylenimine)-Mediated Gene Delivery Affects Endothelial Cell Function and Viability. Biomaterials 2001, 22, 471−480.

55. Yu K, Zhao J, Zhang Z, et al. Enhanced delivery of Paclitaxel using electrostatically-conjugated herceptin-bearing PEI/PLGA nanoparticles against HER-positive breast cancer cells. Int J Pharm. 2016;497(1–2):78–87.

56. Lazarus GS, Cooper DM, Knighton DR, et al. Definitions and Guidelines for Assessment of Wounds and Evaluation of Healing. Arch Dermatol. 1994;130(4):489–493.

57. Ja¨rbrink K, Ni G, So¨nnergren H, et al. The humanistic and economic burden of chronic wounds: a protocol for a systematic review. Syst Rev 2017;6:15–15.

58. Posnett J, Franks PJ. The burden of chronic wounds in the UK. Nurs Times. 2008;104(3):44–5.

59. Rodrigues, M.; Kosaric, N.; Bonham, C.A.; Gurtner, G.C. Wound healing: A cellular perspective. *Physiol. Rev.* 2019, *99*, 665–706.

60. Fife, C.E.; Eckert, K.A.; Carter, M.J. Publicly reported wound healing rates: The fantasy and the reality. *Adv. Wound Care* 2018, *7*, 77–94.

61. Shubhangi Vinayak Agale, "Chronic Leg Ulcers: Epidemiology, Aetiopathogenesis, and Management", Ulcers, vol. 2013, Article ID 413604, 9 pages, 2013.

62. Guo, S., & Dipietro, L. A. (2010). Factors affecting wound healing. Journal of dental research, 89(3), 219–229.

63. Bowler PG, Duerden BI. Wound microbiology and associated approaches to wound management. Clin Microb Rev 2001;14:244–69.

64. S. Guo and L. A. DiPietro, “Factors affecting wound healing,” Journal of Dental Research, vol. 89, no. 3, pp. 219–229, 2010.

65. B. Alberts, A. Johnson, J. Lewis, M. Raff, K. Roberts, and P. Walter, Molecular Biology of The Cell, Garland Science, Taylor Francis, New York, NY, USA, 4th edition, 2002.

66. Berger, A. G., Chou, J. J., & Hammond, P. T. (2021). Approaches to modulate the chronic wound environment using localized nucleic acid delivery. *Advances in Wound Care*, *10*(9), 503-528.

67. Love KT, Mahon KP, Levins CG, et al. Lipid-like materials for low-dose, in vivo gene silencing. Proc Natl Acad Sci U S A 2010;107:1864–1869.

68. U.S. Food and Drug Administration. FDA approves first-of-its kind targeted RNA-based therapy to treat a rare disease. 2019. http://fda.gov/news-events/press-announcements/fda-approves-first-its-kind-targeted-rna-based-therapy-treat-rare-disease (last accessed October 27, 2019).

69. Elangovan, S., D'Mello, S. R., Hong, L., Ross, R. D., Allamargot, C., Dawson, D. V., Stanford, C. M., Johnson, G. K., Sumner, D. R., & Salem, A. K. (2014). The enhancement of bone regeneration by gene activated matrix encoding for platelet derived growth factor. Biomaterials, 35(2), 737–747.

70. Peng L-H, Wei W, Qi X-T, et al. Epidermal stem cells manipulated by pDNA-VEGF165/CYD-PEI nanoparticles loaded gelatin/b-TCP matrix as a therapeutic agent and gene delivery vehicle for wound healing. Mol Pharm 2013;10:3090–3102.

71. Ban E, Jeong S, Park M, et al. Accelerated wound healing in diabetic mice by miRNA-497 and its anti-inflammatory activity. Biomed Pharmacother 2020;121:109613.

72. Whittam AJ, Maan ZN, Duscher D, et al. Challenges and opportunities in drug delivery for wound healing. Adv Wound Care 2016;5: 79–88.

73. MP, Martins VLC, O'Toole EA. Metallo-proteinases and wound healing. Adv Wound Care (New Rochelle) 2015;4:225–234.

74. Friedl, P. and Weigelin, B. (2008) Interstitial leukocyte migration and immune function. Nat. Immunol. 9, 960–969.

75. Hettler A, Werner S, Eick S, Laufer S, Weise F. A new in vitro model to study cellular responses after thermomechanical damage in monolayer cultures. PLoS One. 2013;8:e82635.

76. Liang C-C, Park AY, Guan J-L. In vitro scratch assay: a convenient and inexpensive method for analysis of cell migration in vitro. Nat Protoc. 2007; 2:329–33.

77. Zhang C, Zhai W, Xie Y, Chen Q, Zhu W, Sun X. Mesenchymal stem cells derived from breast cancer tissue promote the proliferation and migration of the MCF-7 cell line in vitro. Oncol Lett. 2013;6:1577–82.

78. Topman G, Sharabani-Yosef O, Gefen A. A standardized objective method for continuously measuring the kinematics of cultures covering a mechanically damaged site. Med Eng Phys. 2012;34:225–32.

79. Klettner A, Tahmaz N, Dithmer M, Richert E, Roider J. Effects of aflibercept on primary RPE cells: toxicity, wound healing, uptake and phagocytosis. Br J Ophthalmol. 2014;98:1448–52.

80. Rodriguez, L.G., Wu, X., Guan, JL. (2005). Wound-Healing Assay. In: Guan, JL. (eds) Cell Migration. Methods in Molecular Biology™, vol 294. Humana Press.

81. Charafeddine RA, Makdisi J, Schairer D, O'Rourke BP, Diaz-Valencia JD, Chouake J, Kutner A, Krausz A, Adler B, Nacharaju P, Liang H, Mukherjee S, Friedman JM, Friedman A, Nosanchuk JD, Sharp DJ. Fidgetin-Like 2: A Microtubule-Based Regulator of Wound Healing. J Invest Dermatol. 2015 Sep;135(9):2309-2318.

82. Bretscher MS (1996) Moving membrane up to the front of migrating cells. Cell 85(4):465 467.

83. Maritzen, T., Schachtner, H. & Legler, D.F. On the move: endocytic trafficking in cell migration. Cell. Mol. Life Sci. 72, 2119–2134 (2015). https://doi.org/10.1007/s00018-015-1855-9.

84. Neel NF, Schutyser E, Sai J, Fan GH, Richmond A (2005) Chemokine receptor internalization and intracellular trafficking. Cytokine Growth Factor Rev 16(6):637–658.

85. Borroni EM, Mantovani A, Locati M, Bonecchi R (2010) Chemokine receptors intracellular trafficking. Pharmacol Ther 127(1):1–8.

86. Stenmark H (2009) Rab GTPases as coordinators of vesicle traffic. Nat Rev Mol Cell Biol 10(8):513–525.

87. Martinez-Arroyo, O., Selma-Soriano, E., Ortega, A., Cortes, R., & Redon, J. (2021). Small Rab GTPases in Intracellular Vesicle Trafficking: The Case of Rab3A/Raphillin-3A Complex in the Kidney. International journal of molecular sciences, 22(14), 7679. https://doi.org/10.3390/ijms22147679

88. Ross, N. L., Munsell, E. V., Sabanayagam, C., & Sullivan, M. O. (2015). Histone-targeted Polyplexes Avoid Endosomal Escape and Enter the Nucleus During Postmitotic Redistribution of ER Membranes. Molecular therapy. Nucleic acids, 4(2), e226. https://doi.org/10.1038/mtna.2015.2

89. Nilesh P. Ingle, Lian Xue, and Theresa M. Reineke. Molecular Pharmaceutics. 2013. 10 (11), 4120-4135. DOI: 10.1021/mp400115y

90. Rink, J, Ghigo, E, Kalaidzidis,Y and Zerial, M (2005). Rab conversion as a mechanism of progression from early to late endosomes. Cell 122: 735–749.

91. Puck T.T., Cieciura Steven J. Genetics of somatic mammalian cells∗ iii. Long-term cultivation of euploidcells from human and animal subjects. J. Exp. Med. 1958;108:945–956.

92. Lee, D. Y., Lee, S. Y., Yun, S. H., Jeong, J. W., Kim, J. H., Kim, H. W., Choi, J. S., Kim, G. D., Joo, S. T., Choi, I., & Hur, S. J. (2022). Review of the Current Research on Fetal Bovine Serum and the Development of Cultured Meat. Food science of animal resources, 42(5), 775–799. https://doi.org/10.5851/kosfa.2022.e46

93. Fasbender, A.; Zabner, J.; Zeiher, B. G.; Welsh, M. J. A Low Rate of Cell Proliferation and Reduced DNA Uptake Limit Cationic Lipid Mediated Gene Transfer to Primary Cultures of Ciliated Human Airway Epithelia. Gene Ther. 1997, 4 (11), 1173−80.

94. Larsen, J. D.; Ross, N. L.; Sullivan, M. O. Requirements for the Nuclear Entry of Polyplexes and Nanoparticles During Mitosis. J. Gene Med. 2012, 14 (9−10), 580−9.

95. Assaker G, Ramel D, Wculek SK, Gonzalez-Gaitan M, Emery G (2010) Spatial restriction of receptor tyrosine kinase activity through a polarized endocytic cycle controls border cell migration. Proc Natl Acad Sci USA 107(52):22558 22563.

96. Kawada K, Upadhyay G, Ferandon S, Janarthanan S, Hall M, Vilardaga JP, Yajnik V (2009) Cell migration is regulated by platelet-derived growth factor receptor endocytosis. Mol Cell Biol 29(16):4508–4518.

97. Ulasov, A. V., Khramtsov, Y. V., Trusov, G. A., Rosenkranz, A. A., Sverdlov, E. D., & Sobolev, A. S. (2011). Properties of PEI-based polyplex nanoparticles that correlate with their transfection efficacy. Molecular therapy : the journal of the American Society of Gene Therapy, 19(1), 103–112. https://doi.org/10.1038/mt.2010.233

98. Forrest, M.L., Koerber, J.T., and Pack, D.W. (2003). A degradable polyethylenimine derivative with low toxicity for highly efficient gene delivery. Bioconjug. Chem. 14, 934–940.

99. Gabrielson, N.P., and Pack, D.W. (2006). Acetylation of polyethylenimine enhances gene delivery via weakened polymer/DNA interactions. Biomacromolecules 7, 2427–2435.

100. Gilleron J, Querbes W, Zeigerer A, et al. Image-based analysis of lipid nanoparticle-mediated siRNA delivery, intracellular trafficking and endosomal escape. Nat Biotechnol 2013; 31: 638-U102.

101. Shi, J., Choi, J. L., Chou, B., Johnson, R. N., Schellinger, J. G., & Pun, S. H. (2013). Effect of polyplex morphology on cellular uptake, intracellular trafficking, and transgene expression. ACS nano, 7(12), 10612–10620. https://doi.org/10.1021/nn403069n

102. Räsänen, K., & Vaheri, A. TGF-beta1 causes epithelial-mesenchymal transition in HaCaT derivatives but induces expression of COX-2 and migration only in benign, not in malignant keratinocytes. Journal of Dermatological Science. 58 (2), 97-104 (2010).

103. Pinilla-Macua, I., & Sorkin, A. (2015). Methods to study endocytic trafficking of the EGF receptor. Sorting and Recycling Endosomes, 347–367. https://doi.org/10.1016/bs.mcb.2015.05.008

104. Vang Mouritzen, M., Jenssen, H. Optimized Scratch Assay for In Vitro Testing of Cell Migration with an Automated Optical Camera. J. Vis. Exp. (138), e57691, doi:10.3791/57691 (2018).

105. Tomasz, M. Mitomycin C: small, fast and deadly (but very selective). Chemistry and Biology. 2 (9), 575-579 (1995).

106. Pezzoli, D., Giupponi, E., Mantovani, D., & Candiani, G. (2017). Size matters for in vitro gene delivery: investigating the relationships among complexation protocol, transfection medium, size and sedimentation. Scientific reports, 7, 44134. https://doi.org/10.1038/srep44134

107. Jonkman, J. E., Cathcart, J. A., Xu, F., Bartolini, M. E., Amon, J. E., Stevens, K. M., & Colarusso, P. (2014). An introduction to the wound healing assay using live cell microscopy. Cell adhesion & migration, 8(5), 440–451. https://doi.org/10.4161/cam.36224

108. Stamm, A., Reimers, K., Strauß, S., Vogt, P., Scheper, T. & Pepelanova, I. (2016). In vitro wound healing assays – state of the art. BioNanoMaterials, 17(1-2), 79-87. https://doi.org/10.1515/bnm-2016-0002

Appendix

Vortex Mixing of PEI-pDNA Nanoparticles

As described in Chapter 2, polyplexes were prepared by vortex mixing, which can be subject to batch-to-batch and intra-batch variability with less control over the physical process of assembly. This can result in non-uniform nanoparticles and poor reproducibility. To ensure that consistent polyplex properties were obtained using vortex mixing, five polyplexes with the same N/P ratio were synthesized following the standard protocol outlined in Chapter 2. The size and polydispersity index were characterized using DLS and the surface charge was measured for each complex. As shown in Figure A-1, all polyplexes formed were under 200 nm in diameter with similar polydispersity indexes. Additionally, Figure A-2 reveals that all PEI-pDNA complexes were positively charged. Therefore, the conventional vortex mixing method used for this study served as an effective method for spontaneously self-assembly of nanoparticles for efficient gene transfection.

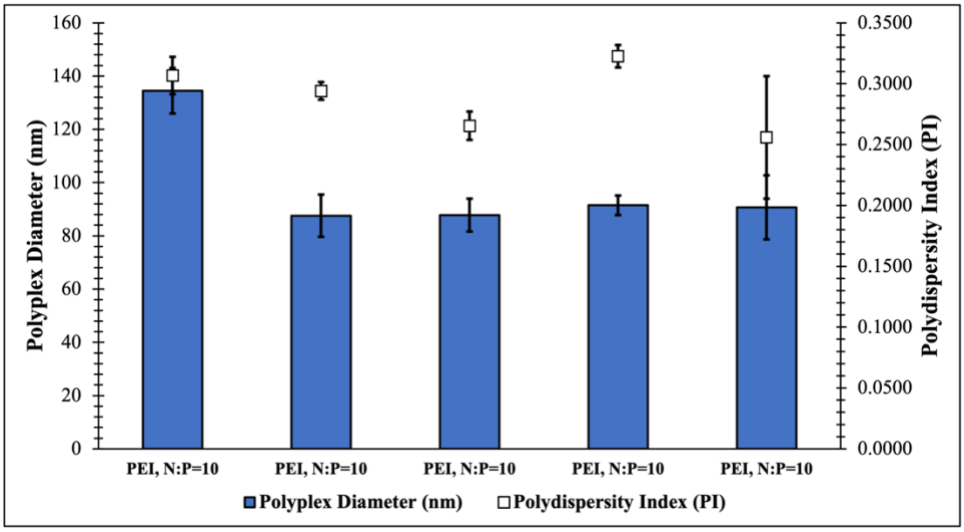

Figure A-1. Average hydrodynamic diameters and polydispersity indexes (associated with secondary y-axis) of N/P 10 polyplexes. Results are shown as the mean ± standard deviation of data obtained from three independent measurements.

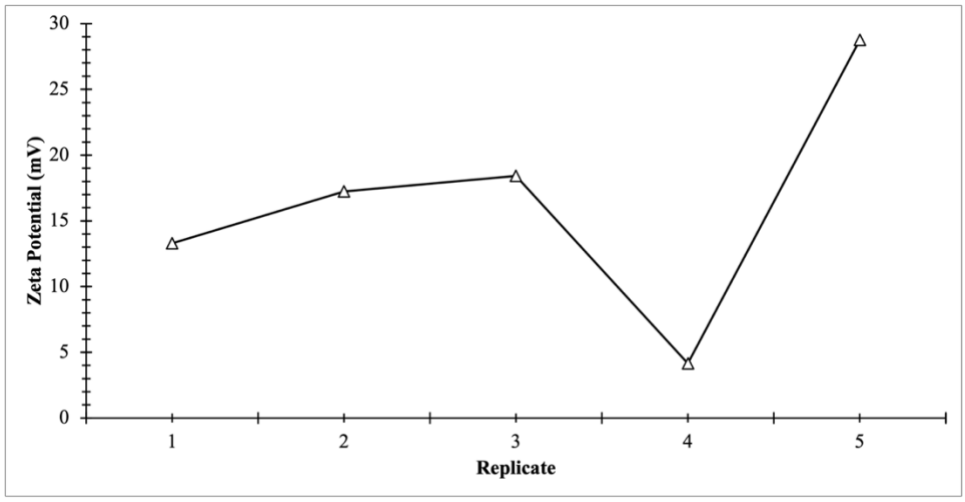

Figure A-2. Average zeta potentials of N/P 10 polyplexes.